Electromagnetic excitations in metals and semimetals in a strong magnetic field

V. Ya. Demikhovskiĭ and A. P. Protogenov

State University and Radiophysics Scientific Research Institute (NIRFI), Gor'kiĭ
Usp. Fiz. Nauk. **118**, 101–139 (January 1976)

Work in which electromagnetic excitations in metals and semimetals in a strong magnetic field have been studied is reviewed. For the analysis of the spectrum of the numerous electromagnetic excitations, the collisionless-damping regimes which determine the limits of the existence of weakly-damped excitations and make it possible to carry out a natural classification of the spectrum of electromagnetic waves in quantizing and classically-strong magnetic fields are derived with the aid of conservation laws. In addition, the collisionless-damping regimes give an intuitive picture of oscillatory effects in the propagation of other, nonelectromagnetic excitations. All types of quantum waves in electron and electron-hole plasmas and also the effect of magnetic quantization on the spectrum of the classical electromagnetic excitations, are considered in the review. The conditions for which quantum waves and oscillations of the damping of classical excitations can be observed are discussed. The last section of the review summarizes the results of work in which electromagnetic waves in metals with a complicated Fermi surface have been studied. The connection between the geometry of the Fermi surface and the spectrum of the electromagnetic normal modes is analyzed.

PACS numbers: 71.90.+q

CONTENTS

1. INTRODUCTION

In the last decade a new area of solid-state physics has been formed—the electrodynamics of conductors situated in a strong magnetic field. The investigations of the electromagnetic-excitation spectrum, which form the basis of this field, are reflected in the well-known reviews[1–4] and monographs.[5–9]

The spectrum of the electromagnetic excitations in classically-strong magnetic fields is extremely diverse in form. In a quantizing magnetic field, because of the multi-component character of the electron-hole system, it becomes more complicated, since, as a rule, new types of collective excitations correspond to the numerous electronic transitions between the Landau levels. Moreover, the quantization entails changes in the spectrum of waves which already exist in classically-strong magnetic fields. In recent years a series of papers have been published in which different types of electromagnetic waves in a quantizing magnetic field have been discovered and studied theoretically.

The spectrum of electromagnetic excitations in solids is intimately connected with the geometry of the Fermi surface. Because of this, in metals and semimetals excitations can propagate that do not exist in a gas-discharge or ionospheric plasma or in metals in which the carriers have an isotropic quadratic spectrum. The problem of the electromagnetic-excitation spectrum in metals having a complex Fermi surface has also attracted the attention of theoreticians and experimentalists in recent years.

Work devoted to the study of electromagnetic waves in both quantizing and classically-strong magnetic fields is included in this review. To investigate the electromagnetic-excitation spectrum we have made use of the conservation laws that are fulfilled when electrons interact with the Bose excitations. With the aid of the conservation laws, the regimes of collisionless damping of excitations interacting with electrons in a magnetic field are derived in the "frequency-wavevector" plane for different models of the electron spectrum. In pure metals and semimetals at sufficiently low temperatures, these regimes determine the limits of existence of undamped collective excitations. Since selection rules establish a connection between the polarization of a wave and the type of resonance transitions between the Landau levels, it is not difficult to determine the regimes of existence of waves with a specific polarization. Using the regimes of transparency a natural classification of the possible solutions of the dispersion equation for waves with a given polarization can thereby be made. To determine the solution it is now sufficient to consider only a certain "window" in the collisionless-damping regimes, in which the analytical expression for the conductivity acquires a sufficiently simple form.

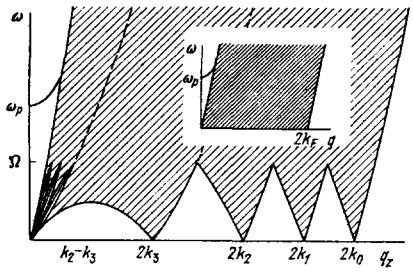

FIG. 1. Landau-damping regimes in a quantizing magnetic field ($\Delta n = 0$). (Four Landau levels are occupied ($n_F = 4$). The spectra of the longitudinal quantum waves and of the plasmon are shown in the figure. The Landau-damping regime in the absence of magnetic quantization is depicted in the upper part of the figure.)

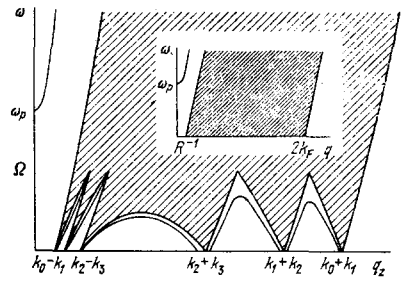

FIG. 3. Regimes of anomalous cyclotron damping in a quantizing magnetic field ($\Delta n = -1$, $n_F = 4$). (The spectra of the right-polarized quantum waves and the high-frequency wave are shown in the figure. The regime of anomalous cyclotron damping in the absence of magnetic quantization is depicted in the upper part of the figure.)

The collisionless-damping regimes also give an intuitive picture of the different resonance effects associated with other elementary excitations. Therefore, such an approach is methodologically appropriate in the study of resonance effects such as giant quantum oscillations of sound absorption, oscillations of the sound velocity, geometric resonance, oscillations of the damping of optical phonons, etc.

The review is constructed as follows. In Sec. 2 we consider the collisionless-damping regimes for excitations of different polarizations. The shift of the damping regimes with change of the magnitude and direction of the magnetic field illustrates the different oscillation effects.

In Sec. 3 the basic equations of the electrodynamics of conductors situated in a quantizing magnetic field are given. The conductivity tensor for electrons in a quantizing field is found. The scales of the space and time dispersion, and also the question of the form of the collision integral, are discussed. In Sec. 4 the spectrum of the electromagnetic excitations in a degenerate magnetically-active plasma is analyzed in the simplest model of a quadratic and isotropic dispersion law for the electrons. All types of classical and quantum waves in electron and electron-hole plasmas are considered. The fine structure of the windows in the collisionless-damping regimes (see Figs. 1–3 below)

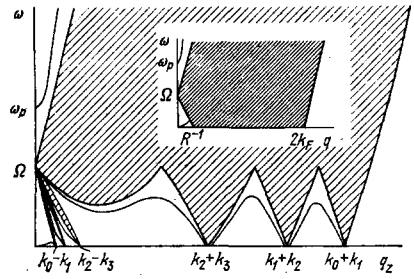

FIG. 2. Cyclotron-damping regimes in a quantizing magnetic field ($\Delta n = 1$, $n_F = 4$). (The spectra of the helicon, the left-polarized quantum waves and the high-frequency left-polarized wave are shown in the figure. The regime of normal cyclotron damping in the absence of magnetic quantization is depicted in the upper part of the figure.)

is extremely sensitive to the thermal smearing-out of the distribution function. In addition, the boundaries of the regimes can be smeared out on account of electron collisions. This leads to damping of the excitations. Each region has its own criterion for weak damping of a wave, imposing bounds on the temperature and collision frequency. In connection with this, the conditions for the existence of quantum waves are discussed.

Section 5 is devoted to a discussion of work in which electromagnetic excitations in metals with a complex Fermi surface have been studied in classically-strong and quantizing magnetic fields. Here, as in the previous sections, we consider the selection rules, the regimes of collisionless damping in metals with an anisotropic spectrum, the singularities of the conductivity tensor, and also the principal types of electromagnetic waves and their connection with the geometry of the Fermi surface. We have directed our attention principally to the origin of the electromagnetic excitations and their classification, without going into the details of the spectrum of the waves.

2. COLLISIONLESS-DAMPING REGIMES

The propagation of electromagnetic excitations in a solid in a classically-strong or quantizing magnetic field is described by the Maxwell equations and the classical or quantum equation of motion of the charged particles. As is well-known, the excitation spectrum is found from the dispersion equation, which, because of the multi-component nature of the system under consideration, the space and time dispersion and the strong anisotropy, turns out to be rather complicated. In order to visualize the entire multiplicity of excitations, in the present section we turn to the conservation laws that are fulfilled when an electron interacts with a Bose excitation. The conservation laws determine the thresholds for creation of electron-hole pairs by different Bose excitations and, consequently, indicate the limits of existence of the undamped excitations. On one side of the threshold—the side where the transitions are virtual—the imaginary part of the dielectric permittivity is equal to zero, and beyond the threshold it is nonzero. By virtue of the Kramers–Krönig dispersion relations this leads to a singularity in the real

part of the dielectric permittivity at the threshold. Therefore, collective excitations whose spectrum lies near the corresponding resonance frequencies can correspond to resonances.

We shall consider the collisionless-damping regimes for an isotropic quadratic electron spectrum. The damping regimes in metals with a complex Fermi surface will be considered in Sec. 5.

In the case when the motion of the electrons is described classically, the mechanism of the collisionless damping can be elucidated in the following way. A longitudinal wave interacts strongly with those particles whose velocity is approximately equal to the phase velocity of the wave. Such particles "see" an almost constant electric field in the wave, while particles moving faster than the wave give up energy to it and particles lagging behind the wave absorb energy. Since in the equilibrium state the number of slow particles is always greater than the number of fast particles, the wave is damped. This mechanism for collisionless damping of longitudinal waves is called Landau damping. If the electron gas is degenerate, the Landau damping has a natural threshold $\omega/q = v_F$.

A circularly polarized wave propagating parallel to a magnetic field can also experience collisionless damping. To understand the physical cause of damping of transverse waves, we change to a system of coordinates in which the velocity of the particle along the magnetic field is equal to zero. If the frequency of the wave in this coordinate system is equal to the frequency of rotation of the electron, the electron "sees" a constant electric field in the wave, lying in the plane of its rotation, and absorbs energy. Such damping is usually called cyclotron damping. In a degenerate electron gas, when the maximum electron velocity is equal to v_F, the thresholds for normal and anomalous cyclotron damping are determined by the condition $\omega = \pm(\Omega \pm v_F q)$.

If the wave propagates at an angle to the direction of the constant magnetic field, the interaction of the particle with the electric and magnetic fields of the wave becomes more complicated. For example, in the propagation of a helicon at an angle to the magnetic-field direction, transfer of energy from the wave to particles occurs on account of the joint action of the variable electric and magnetic fields lying in the plane perpendicular to the constant magnetic field, and the energy of the motion of the particle in the direction of the constant magnetic field is changed. As a result, magnetic Landau damping arises in the region $\omega/q_z < v_F$. [1,9]

We turn now to the quantum interpretation of collisionless damping. An elementary excitation with frequency ω and wave-vector q is damped if it can create an electron-hole pair. This process must be allowed by the conservation laws for the energy and longitudinal component of the momentum:

$$\varepsilon_n(p_z) + \hbar\omega_q = \varepsilon_{n'}(p_z + \hbar q_z), \tag{2.1}$$

where

$$\varepsilon_n(p_z) = \hbar\Omega\left(n + \frac{1}{2}\right) + \frac{p_z^2}{2m} \tag{2.2}$$

is the energy of an electron in the quantizing magnetic field, n labels the Landau level, p_z is the component of the momentum in the magnetic-field direction, $\hbar$ is Planck's constant, Ω is the cyclotron frequency and m is the electron mass.

In addition, for the process to be allowed the Pauli principle must be satisfied: at zero temperature, the electron must be below the Fermi surface in its initial state and must have an energy greater than the Fermi energy in its final state.

In the system under consideration there also exist other conserved quantities, leading to certain selection rules with respect to the quantum number n. If the wave propagates along the magnetic field, then $\Delta n = 0$ for longitudinal polarization of the excitation and $\Delta n = 1$ ($\Delta n = -1$) for a left(right)-polarized excitation. A discussion of the conservation laws from which these selection rules follow is given in [10,11]. If the wave propagates at an angle to the magnetic field, electron transitions with an arbitrary change in the Landau-level number are allowed.

Using the above considerations, we derive the regimes of collisionless damping of elementary excitations in a quantizing magnetic field. For this we solve Eq. (2.1) for p_z and, using the inequalities $\varepsilon_n(p_z) \leqslant \varepsilon_F$, $\varepsilon_{n'}(p_z + \hbar q_z) \geqslant \varepsilon_F$, we find

$$\begin{aligned} \omega &\leqslant \Delta n\Omega \pm v_n q_z \pm \frac{\hbar q_z^2}{2m}, \\ \omega &\geqslant \Delta n\Omega \mp v_n q_z \pm \frac{\hbar q_z^2}{2m}, \end{aligned} \tag{2.3}$$

where $v_n = \sqrt{2[\varepsilon_F - (n+\frac{1}{2})\hbar\Omega]/m}$ is the Fermi velocity at the n-th Landau level and ε_F is the Fermi energy. The inequalities (2.3) determine the collisionless-damping regimes for arbitrary $\Delta n = n' - n$. They are depicted in Figs. 1–3. Fig. 1 shows the collisionless-damping regimes for transitions with no change in the Landau-level number ($\Delta n = 0$); Figs. 2 and 3 correspond to the cases when $\Delta n = 1$ and $\Delta n = -1$.

We shall discuss these figures. The propagation of a longitudinal excitation along the magnetic field in crystals with an isotropic quadratic dispersion law for the electrons is accompanied by transitions with $\Delta n = 0$ and, consequently, the regime of collisionless damping of the excitations will be the region shown in Fig. 1. The dashed lines in the shaded region show the boundaries of the damping for transitions within an individual Landau level ($n = n_F$). The complete picture of the damping is obtained by superimposing the damping regions corresponding to transitions in all Landau levels. As can be seen from the figure, as a result of this superposition "windows" in which damping is absent appear in the (ω, q)-plane. Conventionally, one can distinguish two types of windows. One type emerges from the coordinate origin, and the others are located in the region of larger q up to $2k_F$. It is essential that all windows lie below the cyclotron frequency. The number of areas of transparency of the first type is smaller, by one, than the number of filled Landau levels, and the number of windows bordering on the q-axis is equal to n_F. The characteristic momenta $2\hbar k_n$ defining the lim-

its of the windows at $\omega = 0$ correspond to electron transitions from states with momentum $-\hbar k_n$ to a state with momentum $\hbar k_n$ with no change in energy. For the subsequent discussion, we note that the width of the damping areas is proportional to q^2 for small q. Bordering on the q-axis in the range $(0, 2k_{nF})$ is the transparency regime formed by electron transitions in the highest Landau level. Its height is equal to $\hbar k_{nF}^2/2m$.

The regions derived indicate those values of the frequency and wave-vector at which undamped excitations can exist. These excitations are considered in Sec. 4(A). It should be emphasized that waves do not exist in all the windows. The position of the dispersion curve in the (ω, q)-plane is determined by the dynamics of the motion of the electrons.

The shift of the damping regions with change in the magnitude and direction of the magnetic field illustrates the change in the spectrum of the electromagnetic waves, and the different oscillation effects. On increase of the magnetic field the Fermi momenta $\hbar k_n$ at the individual Landau levels vary in accordance with the law $\hbar k_n = \sqrt{2m[\varepsilon_F - (n+\frac{1}{2})\hbar\Omega]}$. As a result, the dimensions of the windows along the q-axis, and also their height, which is proportional to Ω, increase. When the number of filled levels changes (when $2k_{nF}$ tends to zero) the number of windows changes and the pattern of the damping regions near the coordinate origin changes sharply. This leads to oscillations of the absorption and velocity of a helicon[12] and of sound.[13,14] The shift of the damping regimes on variation of the angle ϑ between q and H reduces, as follows from (2.1), to extending the scale along the q-axis by the factor $\cos^{-1}\vartheta$, and this explains the giant oscillations in the absorption[15] and velocity[16] of sound on variation of ϑ. In discussing other resonance effects[17-19] we shall also turn to Figs. 1–3.

If the excitation has left circular polarization and interacts with electrons, then, as it propagates along the magnetic field, transitions with $\Delta n = 1$ are allowed by the selection rules. The corresponding damping regimes are depicted in Fig. 2. As can be seen from the figure, the pattern of the damping regimes is different in this case. For example, at zero frequency the boundaries of the windows are determined by the difference and sum $\hbar(k_n \pm k_{n+1})$ of the Fermi momenta at neighboring Landau levels. As in the first case, the windows can be divided conventionally into two types: one type begins at $\omega = \Omega$ and $q = 0$, and the others adjoin the q-axis. The total numbers of windows of the two types are $n_F - 2$ and $n_F - 1$, respectively. With increase of the magnetic field the sum $k_n + k_{n+1}$ decreases and the difference $k_n - k_{n+1}$ increases. This determines the change in the pattern of the damping with variation of the magnetic field. Increase of the angle between q and H leads to an extension of the scale along the q-axis by a factor of $\cos^{-1}\vartheta$. At $\vartheta = \pi/2$ the collisionless-damping regimes degenerate into the line $\omega = \Omega$.

Figure 3 shows the collisionless-damping regimes for $\Delta n = -1$ transitions. Such transitions are allowed for right-polarized waves interacting with electrons and propagating along the magnetic field. The structure of the collisionless-damping regimes, as in the preceding two cases, makes it possible to distinguish windows of two types and an intermediate region of transparency. The characteristic momenta and the number of windows are the same as in the case $\Delta n = 1$. However, the form of the damping regimes is different. The regions shown in Figs. 2 and 3 characterize the spectrum of electromagnetic waves in a quantizing field (cf., e.g., Sec. 4(B)) and illustrate the different resonance effects for transversely polarized excitations.

It should be kept in mind that, if a certain excitation with circular polarization interacts not with electrons but with holes, the selection rules allow transitions with $\Delta n = 1$ for right-polarized waves and with $\Delta n = -1$ for excitations with left circular polarization. Therefore, Fig. 2 gives the pattern of the regimes of damping of right-polarized waves in a hole gas and Fig. 3 corresponds to the regimes of damping of left-polarized excitations.

On all the boundaries of the damping regions depicted in Figs. 1–3 the real part of the dielectric permittivity, as will be shown in Sec. 3, has logarithmic singularities while the imaginary part experiences a finite discontinuity.

If the electromagnetic wave propagates at an angle to the magnetic field, transitions with an arbitrary change in the quantum number n are possible. Because of this, the form of the damping regions becomes more complicated, and they can be obtained by a simple superposition of the damping regimes for $\Delta n = 0, \pm 1, \pm 2$, etc. It is not difficult to convince oneself that the damping regions corresponding to transitions $\Delta n = \pm 2, \pm 3, \ldots$ are similar to the regions for $\Delta n = \pm 1$. If we neglect the quantum effects in (2.3), then, for an arbitrary direction of propagation of the wave, the boundaries of the damping regimes have the form $\omega = \Delta n\Omega \pm v_F q$, where $\Delta n = 0, \pm 1, \pm 2, \ldots$ In the upper parts of Figs. 1–3 the damping regimes for longitudinal, left-polarized and right-polarized waves in classically-strong magnetic fields ($\Omega \gg \nu$) are shown. At $\vartheta = \pi/2$ the damping regions are transformed into the lines $\omega = \Delta n\Omega$. Without going into details, we point out that an idea of the collisionless-damping regimes for arbitrary Δn can be obtained from [20]. Waves propagating at an angle to the magnetic-field direction are considered in Sec. 4(D).

We now take the spin splitting into account. It leads to a doubling of the number of magnetic tubes and to a "splitting" of the boundaries of the collisionless-damping regimes. In turn, the latter leads to the appearance of additional excitations and causes splitting of the resonances in the corresponding oscillation effects. The characteristic dimensions of the areas of transparency are determined by the relationship between the cyclotron frequency and the spin frequency[20]

$$\omega_0 = g\mu_0 H,$$

where g is the spin-splitting factor and μ_0 is the Bohr magneton.

In a series of papers, Zyryanov, Okulov and Silin have studied quantum waves in an electron Fermi liquid.

In particular, quantum spin waves were treated in [21-23]. The regimes of collisionless damping of these excitations can be found using the conservation law for processes with change in the projection of the spin. The approach proposed can also be useful for analyzing the spin-wave spectrum. However, spin waves in a Fermi liquid are not considered in this review.

The characteristic sizes and numbers of windows in the damping regimes are essentially different in metals and semimetals. This is connected with the fact that in metals the number of filled levels, even in fields $H \sim 10^5$ Oe, is not less than 10^3–10^4, while in semimetals and semiconductors a few Landau levels may be filled. As a result, in metals it is not possible to resolve all the windows when observing resonance effects. The uncertainty in the energy-conservation law, associated with electron collisions, and the thermal smearing-out of the distribution function lead to blurring of the boundaries of the collisionless-damping regimes and, in weak magnetic fields, to the complete disappearance of the quantization effects. The necessary and sufficient conditions for the existence of the different resonance effects in metals and semimetals, and also the conditions for the observation of quantum electromagnetic waves, will be discussed later. Here, we remark only that if the magnetic-quantization condition

$$T \ll \hbar\Omega, \ \nu \ll \Omega \tag{2.4}$$

is not fulfilled there are no windows in the collisionless-damping regimes. Here, T is the temperature in energy units and ν is the collision frequency.

3. BASIC EQUATIONS

The spectrum of the electromagnetic excitations in conductors in a quantizing magnetic field can be found from Maxwell's equations and the equation for the density matrix:

$$\operatorname{rot} \mathbf{H} = \frac{4\pi}{c}\mathbf{j} + \frac{1}{c}\frac{\partial \mathbf{E}}{\partial t}, \tag{3.1}$$

$$\operatorname{rot} \mathbf{E} = -\frac{1}{c}\frac{\partial \mathbf{H}}{\partial t}, \tag{3.2}$$

$$\frac{\partial \hat{\rho}}{\partial t} + \frac{i}{\hbar}[\hat{\mathcal{H}}, \hat{\rho}] = \left(\frac{\partial \hat{\rho}}{\partial t}\right)_{\text{coll}}; \tag{3.3}$$

here $\mathbf{E}$ and $\mathbf{H}$ are the intensities of the electric and magnetic fields, $\mathbf{j}$ is the current density, c is the velocity of light, $\hat{\rho}$ is the single-particle density matrix and $\hat{\mathcal{H}}$ is the Hamiltonian of the system. Equations (3.1)–(3.3) are connected by

$$\mathbf{j}(\mathbf{r}_0, t) = \operatorname{Sp}\left\{-\frac{1}{2}e\left[\hat{\mathbf{v}}_0 + \frac{e}{mc}\mathbf{A}(\mathbf{r}, t)\right]\delta(\mathbf{r}_0 - \mathbf{r})\hat{\rho} + \text{H.c.}\right\}, \tag{3.4}$$

where $\hat{\mathbf{v}}_0$ is the velocity operator and e is the electron charge. In a constant external magnetic field and in the field of an electromagnetic wave the Hamiltonian of our system has the form

$$\hat{\mathcal{H}} = \frac{1}{2m}\left(\hat{\mathbf{p}} + \frac{e}{c}\mathbf{A}_0 + \frac{e}{c}\mathbf{A}\right)^2 - e\varphi, \tag{3.5}$$

where $\mathbf{A}_0 = (0, Hx, 0)$ and H is the intensity of the constant magnetic field directed along the z-axis; $\mathbf{A}$ and $\varphi \sim \exp[i(\omega t - \mathbf{q}\cdot\mathbf{r})]$ are the vector and scalar potentials of the oscillating electromagnetic field and $\hat{\mathbf{p}} = -i\hbar\nabla$ is the momentum operator. In the approximation linear in $\mathbf{A}$ we have

$$\hat{\mathcal{H}} = \hat{\mathcal{H}}_0 + \hat{\mathcal{H}}_1, \tag{3.6}$$

$$\hat{\mathcal{H}}_0 = m\hat{\mathbf{v}}_0^2/2, \ \hat{\mathcal{H}}_1 = (e/2c)(\hat{\mathbf{v}}_0\mathbf{A} + \mathbf{A}\hat{\mathbf{v}}_0) - e\varphi, \tag{3.7}$$

$$\hat{\mathbf{v}}_0 = \frac{1}{m}\left(\hat{\mathbf{p}} + \frac{e}{c}\mathbf{A}_0\right). \tag{3.8}$$

The eigenfunctions of the operator $\hat{\mathcal{H}}_0$ in the chosen gauge are

$$|\nu\rangle = |n, k_y, k_z\rangle = V^{-1/3}\exp[i(k_y y + k_z z)]\, u_n(x + l_H^2 k_y), \tag{3.9}$$

and the eigenvalues of $\hat{\mathcal{H}}_0$ are given by the expression (2.2). Here V is the normalization volume, $u_n(x)$ is a harmonic-oscillator eigenfunction and $l_H = (c\hbar/eH)^{1/2}$ is the magnetic length. We note that the interaction of the intrinsic magnetic moment of the electron with the constant and oscillating magnetic fields is not taken into account in the Hamiltonian (3.5).

To determine the current it is necessary to solve Eq. (3.3) for the density matrix. First we shall discuss the form of the collision integral. It is shown in [24-26] that in the τ-approximation the collision integral for the system under consideration should be written in the following form:

$$\left(\frac{\partial \hat{\rho}}{\partial t}\right)_{\text{coll}} = -\frac{\hat{\rho} - \hat{\rho}_0(\hat{\mathcal{H}}, \mu)}{\tau}, \tag{3.10}$$

where

$$\hat{\rho}_0(\hat{\mathcal{H}}, \mu) = \left[\exp\left(\frac{\hat{\mathcal{H}} - \mu}{T}\right) + 1\right]^{-1}, \tag{3.11}$$

τ is the constant relaxation time and μ is the local chemical potential, dependent on $\mathbf{r}$ and t, the value of which is determined from the particle-number conservation condition

$$\operatorname{Sp}\{\delta(\mathbf{r} - \mathbf{r}_0)[\hat{\rho}_0(\hat{\mathcal{H}}, \mu) - \hat{\rho}]\} = 0. \tag{3.12}$$

According to (3.10), the nonequilibrium density matrix relaxes to the local-equilibrium density matrix, which depends on the total Hamiltonian and on the local value of μ. The collision integral, as follows from (3.12), conserves the number of particles. The requirements imposed on the form of the collision integral by other local conservation laws have been discussed in [24,27]. We remark that in a quantizing magnetic field the τ-approximation cannot be rigorously justified. In certain cases it gives a clearly incorrect result. For example, it is impossible to obtain by means of the τ-approximation the correct expression for the static conductivity in a quantizing field in a direction perpendicular to $\mathbf{H}$. [28] However, as a rule, the τ-approximation turns out to be adequate for the study of phenomena in the high-frequency regime $\omega\tau \gg 1$.

In order to solve the system (3.1)–(3.3) it is necessary to find the nonequilibrium correction to the density matrix and then, by means of (3.4), determine the current and conductivity tensor. For an arbitrary orientation of the vector with respect to the magnetic field the expression for the current density has a cumbersome form (see the Appendix).

The simplest expressions for the conductivity tensor

σ_{ik} and the diffusion tensor d_{ik} are obtained in the symmetric geometries $\mathbf{q} \parallel \mathbf{H}$ and $\mathbf{q} \perp \mathbf{H}$. In this case, as follows from the formulas given in the Appendix, certain matrix elements and the corresponding components of the tensor vanish.

In this review we shall consider resonance phenomena in the high-frequency regime[1)] $\omega\tau \gg 1$. Therefore, we shall give explicit expressions for the conductivity tensor only for $\omega\tau \gg 1$ and $\mathbf{q} \parallel \mathbf{H}$. [30,31] From the expressions (A. 27)–(A. 30) we have

$$\sigma_{xx} = \sigma_{yy} = \frac{\omega_p^2}{4\pi i\omega}\left[1 + \frac{1}{4\pi^2 l_H^4 n_0 q}(\Sigma_+ + \Sigma_-)\right], \tag{3.13}$$

$$\sigma_{xy} = \frac{\omega_p^2}{16\pi^3 \omega l_H^4 n_0 q}(\Sigma_+ - \Sigma_-), \tag{3.14}$$

$$\sigma_{zz} = -\frac{3\omega_p^2 \omega\Omega}{8\pi i q^3 v_F^3}\Sigma_0, \tag{3.15}$$

$$\Sigma_\pm = \sum_{n=0}^{n_F} \ln\left\{\left[\frac{v_n q - (\hbar q^2/2m) - (\Omega \pm \bar{\omega})}{v_n q + (\hbar q^2/2m) + (\Omega \pm \bar{\omega})}\right]^{n+1}\left[\frac{v_n q - (\hbar q^2/2m) + (\Omega \pm \bar{\omega})}{v_n q + (\hbar q^2/2m) - (\Omega \pm \bar{\omega})}\right]^{n}\right\}, \tag{3.16}$$

$$\Sigma_0 = \sum_{n=0}^{n_F} \ln\left\{\frac{[v_n q - (\hbar q^2/2m)]^2 - \bar{\omega}^2}{[v_n q + (\hbar q^2/2m)]^2 - \bar{\omega}^2}\right\}, \tag{3.17}$$

where $n_F = [(\varepsilon_F/\hbar\Omega) - \frac{1}{2}]$ is the number of filled Landau levels ($[x]$ is the integer part of x). For $\tau \to \infty$ the imaginary part of Σ_0 is equal to π in the collisionless-damping regimes shown in Figs. 1–3. It can be seen from the expressions (3.13), (3.15) and (3.16), (3.17) that, in accordance with the selection rules discussed in Sec. 2, transitions in which the Landau-level number changes by unity ($\Delta n = \pm 1$) make a contribution to the components σ_{xx} and σ_{xy}, while transitions with no change in the Landau-level number ($\Delta n = 0$) contribute to the longitudinal component of the conductivity tensor.

The system under consideration is characterized by a large number of resonance frequencies and wave-vector values, this being connected with the multi-component character of the system. The resonance values of the longitudinal component of the wave-vector (2.3), which are obtained from the conservation laws for the energy and the longitudinal component of the momentum, determine the position of the logarithmic singularities of the conductivity-tensor components (3.13)–(3.15). Resonance values also exist for the transverse component of the wave-vector. Because of the absence of exact conservation of this component, the character of the resonances here is different: instead of the logarithmic singularities, maxima of the function $f_{n,n+\Delta n}$ arise at the resonance values of $q_\perp$. The function $f_{n,n+\Delta n}$ has a maximum at $q_\perp \approx R^{-1} = \Omega/v_F$ if $n = n_F$, $\Delta n = 1$, or at $q_\perp \approx l_H^{-1}$ if $n = 1$, $\Delta n = 1$, or at $q_\perp \approx k_F$ if $n = 1$, $\Delta n = n_F$. One can convince oneself of this by considering the explicit expression (A. 18) for the function $f_{n,n+\Delta n}$. We return to Eqs. (3.1) and (3.2). Eliminating the magnetic field, after Fourier transformation we obtain

$$\left[\frac{c^2 q^2}{\omega^2}\delta_{ik} - \frac{c^2 q_i q_k}{\omega^2} - \varepsilon_{ik}(\omega, q)\right] E_k(\omega, q) = 0, \tag{3.18}$$

where

$$\varepsilon_{ik}(\omega, q) = \delta_{ik} + \frac{4\pi}{i\omega}(\sigma_{ik}(\omega, q) + d_{ik}(\omega, q)) \tag{3.19}$$

is the dielectric permittivity of the system. From (3.18) follows the dispersion equation determining the spectrum of the electromagnetic excitations in conductors in a strong magnetic field:

$$\mathrm{Det}\left|\frac{c^2 q^2}{\omega^2}\delta_{ik} - \frac{c^2 q_i q_k}{\omega^2} - \varepsilon_{ik}(\omega, q)\right| = 0. \tag{3.20}$$

In the following sections the different solutions of the dispersion equation (3.20) will be discussed.

4. CLASSIFICATION OF ELECTROMAGNETIC EXCITATIONS

The collisionless-damping regimes derived in Sec. 2 determine the limits of the existence of undamped electromagnetic waves and make it possible to carry out a classification of them in the simplest, isotropic model of the electron spectrum. Such a model cannot be used to calculate the excitation spectrum in real metals. However, an investigation of this kind is necessary for an understanding of the general structure of the spectrum of electromagnetic waves.

A. Longitudinal electromagnetic waves

First we shall consider longitudinal waves propagating along the magnetic field. The collisionless-damping regimes for these are shown in Fig. 1. In the unshaded regions the imaginary part of the longitudinal dielectric permittivity is equal to zero and (according to (3.15) and (3.20)) the dispersion equation for $\tau^{-1} = 0$ has the form

$$\varepsilon_{zz} = 0, \tag{4.1}$$

$$\frac{q^2}{4\pi e^2} = \frac{m}{4\pi^2 \hbar^2 l_H^2 q}\sum_{n=0}^{n_F} \ln\left|\frac{[v_n q - (\hbar q^2/2m)]^2 - \omega^2}{[v_n q + (\hbar q^2/2m)]^2 - \omega^2}\right|. \tag{4.2}$$

A solution of Eq. (4.2) does not exist in all windows. At a fixed frequency the left-hand side of Eq. (4.2) is a monotonic function of q. Therefore, if the right-hand side of (4.2) varies from $-\infty$ to $+\infty$ with variation of the wave-vector within a certain window, a solution exists in the window. Such a situation is realized in the windows located near the coordinate origin. If the sign of the singularity of the right-hand side is the same along the boundaries of a window, a solution may not exist. The windows bordering on the q-axis, where there is no solution of the dispersion equation, are an example of this.

As shown in [32,33], the solutions for $qR \ll 1$ and $\omega < \Omega$ have the form (cf. also [34,35])

$$\omega = u_n q, \quad u_n = v_n + \alpha v_{n_F}^2/v_F, \tag{4.3}$$

where α ranges from unity, if $v_n \approx v_F$, to $\frac{1}{2}$, if $v_n \approx v_{n_F}$; $v_{n_F} = \hbar\Omega/m$, $0 < n < n_F$. The excitations (4.3) are usually called longitudinal quantum waves. We note that for $n \lesssim n_F$ the deviation δu_n of the velocity (4.3) of the longitudinal quantum wave from v_n is much smaller than the spacing δv_n between neighboring Fermi velocities in the Landau levels, i.e., the dispersion curve passes near the lower boundary of the window. If n

[1)] In the low-frequency regime $\omega\tau \ll 1$, using formulas (A. 25) and (A. 26) one can obtain the correct criterion for the existence of giant quantum oscillations of the coefficient of absorption of a helicon and of sound. [29]

$\ll n_F$, then $\delta u_n \sim \delta v_n$. In the region of large ω it is not possible to obtain so simple an analytical expression. However, it is clear that a solution exists in each window up to $\omega = \Omega$ and $q = k_n - k_{n+1}$. The number of branches in correspondence with the number of windows, is one less than the number of filled Landau levels. The spectrum (4.3) of the longitudinal quantum waves is shown in Fig. 1. The existence of plasma waves of the acoustic type in a charged Fermi system is connected, obviously, with the multi-component character of the system. Relative oscillations of the components, with no essential change in the total charge density, are possible only in this case.

When the temperature and mean free path are finite the longitudinal quantum waves are damped. The damping of the excitations will be small if the dispersion curve is distant from the boundary of the collisionless-damping regime by an amount greater than the distance over which the damping region is smeared out. From this follow the conditions for weak damping in the n-th window[33]:

$$T \ll \frac{\hbar\Omega}{\sqrt{n}}, \quad \nu \ll \frac{\omega\sqrt{n}}{n_F}, \tag{4.4}$$

which are valid in the region $qR \ll n^{-1/2} \sim v_n/v_F$. It can be seen from (4.4) that the conditions for the existence of weakly damped waves in different windows are not the same. The bounds on the temperature and collision frequency depend in different ways on the Landau-level number n and n_F. It is clear that the most favorable conditions are realized in semimetals, when $n_F \gtrsim 1$.

In addition to the quasi-neutral oscillations (4.3), in the system under consideration there exists at $\omega > v_0 q$ the well-known solution of Eq. (4.1)—the plasmon. When the plasmon propagates along **H**, the region of its existence is the same as in the absence of the field, if we disregard the weak oscillations of the velocity v_0. The spectrum of the longitudinal plasma oscillations has been studied in [36,37]. The influence of the magnetic quantization on the plasmon reduces to small corrections ($\sim \hbar\Omega/\varepsilon_F$)[37] in the coefficient of q^2 that takes the spatial dispersion into account, if $q \ll \omega_p/v_F$ and $\mathbf{q} \parallel \mathbf{H}$. In this geometry the limiting frequency $\omega(0)$ does not depend on the magnetic field.

It is not only the spectrum of the electromagnetic natural oscillations in unbounded space that is shaped by the singularities of the dielectric permittivity. In boundary problems these singularities lead to the phenomena of anomalous penetration of an external field into the conductor. The strengthening of the singularity of the dielectric permittivity in a quantizing field substantially alters the screening of the electric field. As shown in the paper[38], at large distances the potential of a constant electric field falls off like

$$\varphi(z) \sim \sum_{n=0}^{n_F} \frac{a_n \sin 2k_n z}{z}, \tag{4.5}$$

where z is the distance from the surface of the conductor and the magnetic field is directed along the z-axis. Thus, if the frequency of the external field is equal to zero, the period of the Friedel oscillations (4.5) is determined by the height $2k_n$ of the Landau tubes. It is at these values of q that the dielectric permittivity $\varepsilon_{zz}(0, q)$ has singularities (see Fig. 1). The screening of the field of a point charge in a quantizing magnetic field was considered in [39,40].

B. Transverse electromagnetic waves

We turn to the discussion of the dispersion law for circularly polarized electromagnetic waves in a quantizing magnetic field. According to (3.13)–(3.20), the dispersion equation for these in the regions where damping is absent (cf. Figs. 2, 3) has, for $\tau^{-1} = 0$, the form

$$\varepsilon_{\mp} = \frac{c^2q^2}{\omega^2}, \tag{4.6}$$

$$\sum_{n=0}^{n_F} \ln\left\{\left|\frac{v_n q \pm (\hbar q^2/2m) \pm (\Omega \mp \omega)}{v_n q - (\hbar q^2/2m) - (\Omega \mp \omega)}\right|^{n+1} \left|\frac{v_n q \pm (\hbar q^2/2m) - (\Omega \mp \omega)}{v_n q - (\hbar q^2/2m) + (\Omega \mp \omega)}\right|^{n}\right\} = 4\pi^2 n_0 l_H q \left(1 + \frac{c^2q^2}{\omega_p^2} - \frac{\omega^2}{\omega_p^2}\right), \tag{4.7}$$

where the signs + and − correspond to right- and left-polarized waves. In accordance with the selection rules, transitions with $\Delta n = -1$ and $\Delta n = 1$ give a contribution to the dispersion equation for right- and left-polarized waves.

First we consider left-polarized waves. In the region $\omega < \Omega - v_0 q + \hbar q^2/2m$ there exists the well-known left-polarized excitation—the helicon.[41] For $qR \ll 1$ and $\omega \ll \Omega$ the spectrum of the wave, as follows from (4.7), has the form

$$\omega = \frac{\Omega}{\omega_p^2} c^2 q^2. \tag{4.8}$$

The conditions for observation of helicons can be fulfilled comparatively easily in pure metals and doped semimetals and semiconductors, since the damping as a result of collisions is proportional to ν/Ω and there is no collisionless damping for $\mathbf{q} \parallel \mathbf{H}$. A detailed analysis of work devoted to the study of helicons in solids is contained in the review by Maxfield,[2] to which we refer the reader who is interested in the details.

If the helicon frequency approaches the collisionless-damping threshold $\omega = \Omega - v_0 q + \hbar q^2/2m$ (see Fig. 2), spatial dispersion of the dielectric-permittivity tensor becomes important and the dispersion dependence $\omega(q)$ becomes more complicated. In metals, this happens at $qR \sim 1$, and in semimetals at $qR \ll 1$. In nonquantizing fields, at the threshold there exists a weak (Kohn) singularity in the helicon spectrum.[1]

Beyond the threshold there exist the left-polarized quantum waves first studied in the work of Glick and Callen.[42] In order to convince oneself of the existence of a solution of Eq. (4.7) in each window, it is sufficient, as in the case of longitudinal quantum waves, to analyze the variation of the sign of the logarithmic singularities on the boundaries of the windows at a fixed frequency. To obtain an analytical expression it is necessary to separate out the resonance terms in the left-hand side of (4.7) and take the contribution of the other terms into account by replacing the summation over n by an integration. The authors of the aforemen-

tioned paper[42] confined themselves to a graphical investigation of the dispersion equation (4.7). Analytical expressions for the spectrum of left-polarized quantum waves for $qR \ll 1$ and $\omega \sim \Omega$ are given in [22]. We shall not give the rather cumbersome analytical expressions for the spectrum, but, following [42], we depict the solutions schematically in Fig. 2.

The dispersion branches are furthest from the damping boundaries in the windows associated with transitions between Landau levels with $n \sim n_F$, and, at frequencies corresponding to the frequencies of a helicon continued beyond the classical damping threshold, the solution passes approximately through the middle of a window. Unlike the longitudinal quantum waves, left-polarized quantum waves exist in all the windows, including when q is of the order of $2k_0$.[20] The frequency of the quantum waves in these regions vanishes near the points $q = k_n + k_{n+1}$.

We shall consider the spectrum of right-polarized excitations. The pattern of the collisionless-damping regimes (see Fig. 3) tells us the regions of the (ω, q)-plane in which solutions are possible. As is well-known, for $qR \ll 1$ for left- and right-polarized waves there exists a high-frequency solution of the dispersion equation (4.6):

$$\omega^2 = \omega_p^2 + c^2 q^2. \tag{4.9}$$

This wave belongs to the region $\omega > v_F q - \Omega$ and, therefore, does not experience collisionless damping. In the region of frequencies $\omega \leqslant \Omega$ in nonquantizing fields a right-polarized excitation does not exist.

As can be seen from Fig. 3, for $qR > 1$ and $\omega < \Omega$ right-polarized quantum waves can exist in quantizing magnetic fields.[43] An investigation of the sign of the logarithmic singularities of the left-hand side of Eq. (4.7) shows that they exist in all windows in the range $R^{-1} < q < 2k_0$ at frequencies $\omega < \Omega$. It is not difficult to obtain an analytical expression for the spectrum of the right-polarized quantum waves near $q = k_n - k_{n+1}$ by separating out the resonance term in Eq. (4.7):

$$\omega_n(q) = v_n \tilde{q} - (v_{n-1} - v_n)\,\tilde{q} \exp\left[-\frac{f(q)}{n}\right]; \tag{4.10}$$

here $f(q) = 4\pi^2 l_H^4 n_0 q$ and $\tilde{q} = q - (k_n - k_{n+1})$. In correspondence with the number of windows, the number of solutions of (4.10) is equal to $n_F - 1$. The schematic form of the solutions in other regions is shown in Fig. 3.

The conditions for observing right-polarized quantum waves can be found in the same way as for longitudinal excitations: the distance in frequency between the dispersion curve and the nearest threshold should be greater than the thermal and impurity broadening of the threshold. This leads to the following inequalities

$$T \ll \hbar\Omega \exp\left[-\frac{f(q)}{n}\right], \quad \nu \ll \Omega \frac{\tilde{q}}{k_n} \exp\left[-\frac{f(q)}{n}\right]. \tag{4.11}$$

We note that the conditions for observing left-polarized waves at the frequencies of a helicon continued beyond the damping threshold are less stringent than (4.11).

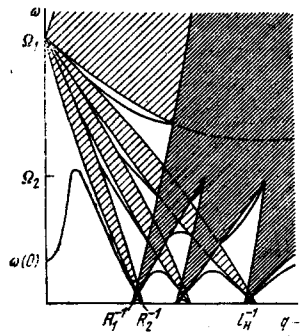

FIG. 4. Spectrum and regimes of collisionless damping of left-polarized electromagnetic waves in an electron-hole plasma in a quantizing magnetic field ($n_2 > n_1$). (The dispersion curves of the quantum waves are shown, as is the excitation (4.16), which goes over into a fast magnetosonic wave and then into a quantum doppleron.)

The conditions (4.11) can be satisfied in pure metals and semimetals at temperatures $T \lesssim 1$ K, collision frequencies $\nu \sim 10^9$ sec^{-1} and wave frequencies $\omega \gtrsim 10^{11}$ sec^{-1}. The magnetic field in semimetals can be of the order of 10^4–10^5 Oe, while in metals stronger magnetic fields ($H \gtrsim 3 \times 10^5$ Oe) are necessary. Evidently, the means for observing right- and left-polarized quantum waves should be different in metals and semimetals. In a metal, in which the skin-depth $\delta \sim 10^{-6}$ cm, quantum waves with $q \sim l_H^{-1}$ ($H > 10^5$ Oe) should be efficiently excited. In this case surface-impedance singularities associated with resonance excitation of the quantum waves will be observed. A detailed theory of such oscillations of the surface impedance is lacking at the present time. In semimetals the skin-depth is of the order of 10^{-4} cm and quantum waves are inefficiently excited. Therefore, the method of study can be based on the phenomenon of the resonance interaction of the transverse quantum waves with high-frequency ($\omega \gtrsim 10^{11}$ sec^{-1}) acoustic phonons[44] or other excitations.

It is well-known[45] that singularities of the dielectric permittivity for $\mathbf{q} \parallel \mathbf{H}$ lead to the phenomena of anomalous penetration of the electromagnetic field (of the trajectory type). The phenomenon of anomalous penetration of the field in classically-strong magnetic fields was predicted in [46]. The numerous thresholds for collisionless damping of transverse waves, which are shown in Figs. 2 and 3 and which correspond to singularities of the dielectric permittivity $\varepsilon_\mp$, clearly indicate the existence of analogous effects in a quantizing magnetic field. However, a detailed calculation of these effects has not yet been carried out.

C. Waves in an electron-hole plasma

In this section we shall discuss the spectrum of electromagnetic excitations in a two-component electron-hole plasma. The spectrum of the transverse waves and the regions of their existence are shown in Figs. 4 and 5. First we consider the solutions in the classical region $qR \ll 1$. The dispersion equation for transverse electromagnetic waves propagating along the magnetic field,

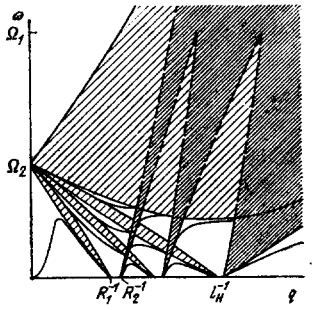

FIG. 5. Spectrum and regimes of collisionless damping of right-polarized electromagnetic waves in an electron-hole plasma in a quantizing magnetic field ($n_2 > n_1$). (The dispersion curves of the quantum waves and of the helicon, which goes over into an Alfven wave and then into a quantum doppleron, are shown.)

$$\sum_{e,h} \varepsilon_{\mp} = \frac{c^2 q^2}{\omega^2}, \tag{4.12}$$

can be written in the following form:

$$\omega_{p_1}^2 \frac{\Omega_1}{\Omega_1 \mp \omega} + \omega_{p_2}^2 \frac{\Omega_2}{\Omega_2 \pm \omega} = \omega_{p_1}^2 + \omega_{p_2}^2 + c^2 q^2 - \omega^2. \tag{4.13}$$

The subscripts 1 and 2 correspond to electrons and holes, and the upper (lower) sign corresponds to left (right) circular polarization of the wave.

If the electron and hole concentrations are not equal, the solutions of Eq. (4.13) for the condition

$$q^2 \ll q_h^2 = \frac{4\pi e^2 (n_1 - n_2)^2}{c^2 (n_1 m_2 + n_2 m_1)} \tag{4.14}$$

are the helicon

$$\omega = \frac{cHq^2}{4\pi e |n_1 - n_2|}, \tag{4.15}$$

and an excitation with the opposite polarization[47]:

$$\omega(q) = \frac{eH}{c} \frac{|n_1 - n_2|}{m_2 n_1 + m_1 n_2} + \frac{n_1 m_1 + n_2 m_2}{n_1 m_2 + n_2 m_1} \cdot \frac{cHq^2}{4\pi e |n_1 - n_2|}. \tag{4.16}$$

The damping constant of the helicon is equal to

$$\gamma = \frac{n_1 m_1 - n_2 m_2}{n_1 m_2 - n_2 m_1} \frac{\nu_{\text{eff}}}{\omega(0)}, \tag{4.17}$$

while for the excitation (4.16),

$$\gamma = \frac{\nu_{\text{eff}}}{\omega}, \tag{4.18}$$

where

$$\nu_{\text{eff}} = \frac{\nu_1 m_1 n_1 + \nu_2 m_2 n_2}{m_1 n_1 + m_2 n_2}. \tag{4.19}$$

The limiting frequency $\omega(0)$ of the wave (4.16) is proportional to the imbalance $n_2 - n_1$, and the coefficient of q^2 differs from the corresponding coefficient in the helicon spectrum by the factor $(n_1 m_1 + n_2 m_2)/(n_1 m_2 + n_2 m_1)$. The polarization of the excitation (4.16) is opposite to that of the helicon: the wave is right-polarized in an electron ($n_1 > n_2$) plasma and has left circular polarization in a hole plasma ($n_2 > n_1$).

If the electron and hole concentrations are equal, the solution of Eq. (4.13) is an Alfven wave and a fast magnetosonic wave, which, for $\omega \ll \Omega_{1,2}$, as is well-known, have the same dispersion law

$$\omega = v_\alpha q, \qquad v_\alpha = \frac{H}{\sqrt{4\pi n (m_1 + m_2)}}, \tag{4.20}$$

and damping constant equal to

$$\gamma = \frac{\nu_{\text{eff}}}{\omega}, \tag{4.21}$$

$$\nu_{\text{eff}} = \frac{\nu_1 m_1 + \nu_2 m_2}{m_1 + m_2}. \tag{4.22}$$

The theoretical and experimental work devoted to the study of Alfven waves in semimetals is reflected in the review by Edel'man.[4]

In uncompensated semimetals, in the region $q_h \ll q \ll R^{-1}$ a helicon goes over into an Alfven wave, and the excitation (4.16) into a fast magnetosonic wave. The change from a helicon spectrum to an Alfven spectrum has been studied experimentally in uncompensated bismuth in [48]. The wave (4.16) has not yet been observed. Apparently, this is the only excitation in the classical regime that has not been detected experimentally.

In the region of strong space and time dispersion the spectrum of the considered excitations in quantizing fields undergoes substantial changes. Near the electron and hole collisionless-damping thresholds (cf. Figs. 4 and 5) new branches—quantum dopplerons, appear in the spectrum.[49] Unlike dopplerons in metals with a complicated Fermi surface (see Sec. 5) a quantum doppleron arises because of the strengthening of the singularity at the damping threshold in a quantizing magnetic field. Estimates show that it is perfectly possible for a quantum doppleron to be observed in semimetals, e.g., in bismuth in fields $H \sim 10^4$–10^5 Oe and at temperatures $T \lesssim 1$ K.

The character of the spectrum of the quantum waves that exist in a two-component plasma beyond the classical damping-boundary $\omega = \pm(\Omega - v_F q)$ is illustrated by Figs. 4 and 5. The collisionless-damping regimes shown in Figs. 4 and 5 are derived taking into account the electron and hole transitions that are allowed for left- and right-polarized waves with $\mathbf{q} \parallel \mathbf{H}$. Longitudinal quantum waves in a two-component plasma have been studied in the work of Konstantinov and Perel'.[33] The differences from the case of a one-component plasma reduce entirely to the appearance of a second series of longitudinal quantum waves, associated with the hole system. We note also that in a two-component system there exists the longitudinal Pines–Schrieffer wave,[50, 51] which can experience giant quantum oscillations of the damping.

D. Electromagnetic excitations propagating at an angle to the magnetic-field direction

It is well-known that electromagnetic excitations propagating at an angle to the magnetic-field direction differ substantially from excitations with $\mathbf{q} \parallel \mathbf{H}$. Indeed, the polarization, spectrum and damping are changed and new branches appear. The corresponding dispersion equations acquire an extremely complicated form. Therefore, to study the solutions it is useful to turn again to the conservation laws.

In the propagation of electromagnetic waves at an angle to the magnetic-field direction, transitions with

arbitrary Δn occur. Additional resonances arise as a consequence of the nonuniformity of the electric and magnetic fields of the wave in the plane perpendicular to H. The collisionless-damping regimes in this case are obtained as a result of superimposing the damping regimes corresponding to all possible transitions between Landau levels. Because of this, the regions of existence of the electromagnetic excitations are changed (they decrease). The points at which the branches of the spectrum of quantum waves terminate can be found without solving the dispersion equation. For this it is necessary only to determine the points of intersection of damping boundaries having dielectric-permittivity singularities of opposite signs. The essential point is that three types of quantum wave exist in each window. By carrying out an investigation of the singularities of the different components of the conductivity tensor in the dispersion equation, it can be shown that in windows associated with, e.g., transitions $\Delta n = 0$, solutions corresponding to one almost longitudinal and two almost transverse polarizations arise. In this case it turns out that the dispersion curves of the transverse waves are positioned nearer to the boundaries than are the dispersion curves of the longitudinal quantum waves. Here we shall not analyze the general case, but confine ourselves to discussing some of the most important effects.

The most interesting effects are those associated with the influence of the magnetic quantization on the spectrum of the classical electromagnetic waves: the helicon and the Alfven and fast magnetosonic waves. In the region of existence of the waves ($\omega < \Omega - v_F q$) these effects are associated with resonances $\Delta n = 0$ (see Fig. 1). In [12], giant quantum oscillations of the damping of helicons were predicted and the conditions for observing the oscillations were carefully analyzed. Experimentally, these oscillations were first observed in aluminum. [52] The interaction between a helicon propagating at an angle to the magnetic field and longitudinal quantum waves was studied in [53], where it was shown that quantum waves whose velocities are close to the phase velocity of the helicon change their polarization and become almost transverse.

We now discuss the effect of quantization on the spectrum of the Alfven and fast magnetosonic waves. In semimetals, because of the low carrier concentration, according to (4.20) the velocities of these waves are greater than the Fermi velocity and, therefore, resonance interaction with electrons with no change in the Landau-level number ($\Delta n = 0$) is absent. In compensated metals in real magnetic fields, $v_\alpha \ll v_F$. For this reason, without magnetic quantization Alfven waves in metals are unobservable even for $\mathbf{q} \parallel \mathbf{H}$, since, for an arbitrary orientation of H with respect to the crystallographic axes, Landau damping exists because of the anisotropy of the electron spectrum.

It was shown in [49] that, in a quantizing field, Alfven and fast magnetosonic waves can propagate if they lie in the windows depicted in Fig. 1, i.e., if their velocity belongs to one of the intervals ($v_n \cos\vartheta$, $v_{n-1}\cos\vartheta$). With change in the angle between q and H, the velocity of a fast magnetosonic wave remains constant but the damping regions are shifted, as was shown in Sec. 2. If the velocity of the wave falls in the intervals $\Delta v_n = \hbar q \cos\vartheta / m$, the fast magnetosonic wave is damped. The velocity of an Alfven wave is proportional to $\cos\vartheta$, and therefore, having fallen in a region of transparency, this wave does not experience giant oscillations of the damping with change of the angle.

Inasmuch as the Alfven and Fermi velocities at the n-th Landau level are different functions of H, for Alfven and fast magnetosonic waves giant oscillations in the absorption will also be observed on variation of the magnetic field. The period of the angular giant oscillations in the absorption of a fast magnetosonic wave is equal to

$$\Delta\vartheta = \operatorname{ctg}\vartheta \cos^2\vartheta \frac{v^2_{n_{F1}}}{v^2_\alpha}, \tag{4.23}$$

and the period in the magnetic field, for Alfven and fast magnetosonic waves, is

$$\Delta H_{1,2} = \frac{H}{n_F + (v^2_{\alpha 1,2}/v^2_{n_{F1}})}, \tag{4.24}$$

where $\cos\vartheta > v_\alpha / v_{F1}$, $v^2_{n_{F1}} = \hbar\Omega_1 / m_1$, $v^2_{\alpha 1} = v^2_\alpha \cos^2\vartheta$ and $v^2_{\alpha 2} = v^2_\alpha$. We note that angular oscillations of the damping and velocity, analogous to (4.23), also exist in the propagation of sound oscillations. [15,16] The dependence of the period in H (4.24) of the giant quantum oscillations differs substantially from the corresponding dependences in de Haas–van Alphen oscillations and in the giant oscillations of Gurevich, Skobov and Firsov. The angular oscillations of a fast magnetosonic wave cease at angles $\cos\vartheta \leqslant v_\alpha / v_{F1}$. The propagation of a fast magnetosonic wave in this range of angles, without magnetic quantization, was considered by Skobov. [54] The criterion for the existence of giant oscillations of the absorption of fast magnetosonic and Alfven waves in a metal can be found if we require that the thermal and impurity spread ($T/m_1 v_{n1}$ and ν/q) in the longitudinal electron velocity be small compared with the interval δv_{n1}. Taking into account that $\delta v_{n1} = \hbar\Omega_1 / m_1 v_{n1}$ ($\delta v_{01} = \hbar\Omega_1 / m_1 v_{F1}$ for $n \sim 1$ and $\delta v_{n_F} = \hbar l_H^{-1} / m$ for $n \sim n_F$), we obtain

$$T \ll \hbar\Omega_1, \quad \nu_1 \ll \omega \frac{v^2_{n_{F1}}}{v^2_\alpha}. \tag{4.25}$$

We note that these conditions are weaker than the conditions (4.4) for observation of longitudinal quantum waves. The conditions (4.25) can be satisfied in pure metals, where $\nu \sim 10^8 - 10^9$ sec^{-1}, in magnetic fields $H \sim 10^5$ Oe and at wave frequencies $\omega \sim 10^{11} - 10^{12}$ sec^{-1}. We recall that to study Alfven waves in metals it is necessary that the thickness of the plate in which the standing wave can be observed be less than $(\operatorname{Im} q)^{-1} = v_\alpha / \nu_{eff}$, and this creates additional difficulties. [4]

For $\vartheta = \pi/2$, as already pointed out, transitions with arbitrary Δn are allowed. The energy conservation law in this case has the form $\omega = \Delta n \Omega$ and, therefore, the damping regimes degenerate into a series of lines. Of the classical waves the ones that survive are the fast magnetosonic wave in a compensated plasma and the excitation (4.16), if $n_1 \neq n_2$. [1,49] In addition, near

the cyclotron-resonance lines $\omega = \Delta n \Omega_{s,h}$ there exist the longitudinal and transverse cyclotron waves that were described in detail in the well-known review by Kaner and Skobov.[1] These waves arise as a consequence of the power singularities of components of the conductivity tensor at $\omega = \Delta n \Omega$. A graphical illustration of the spectrum of the waves, and also of the damping regimes in metals with isotropic and anisotropic electron dispersion laws, is given in the review[1].

The spectrum of electromagnetic waves propagating at an angle to the magnetic-field direction reflects the singularities of the conductivity tensor that are associated with the approximate character of the conservation law for the transverse component of the momentum. The dependence of the conductivity on $q_\perp$ is contained in the matrix elements in (A.10), and the resonance values of $q_\perp$ correspond to the spacing between the Landau tubes in a direction perpendicular to H (cf. Sec. 3). Because of this, the frequency and damping of waves propagating at an angle to the magnetic-field direction have an oscillatory dependence on $q_\perp$. Such oscillations are usually called geometric. Geometric oscillations in the spectrum of cyclotron waves were studied in [55]. For an arbitrary orientation of q with respect to H, resonance effects associated with the exact conservation laws for the energy and longitudinal component of momentum and, simultaneously, with the approximate conservation law for the transverse component of momentum are also possible. It the angle ϑ is close to $\pi/2$, then, in the region $\omega < v_F q \cos\vartheta$ in a nonquantizing magnetic field, for $qR = \pi(n + \frac{1}{4})$, when the matrix element vanishes, collisionless Landau damping is absent. At such values of q, as shown in the paper[56] by Kaner and Skobov, waves with a discrete spectrum can exist. Effectively, these waves are the continuation, into the short-wavelength part of the spectrum, of a helicon propatating in a direction almost perpendicular to H. A detailed description of the dispersion and damping of waves with a discrete spectrum is given in the review[1].

5. ELECTROMAGNETIC WAVES IN METALS WITH AN ANISOTROPIC ELECTRON SPECTRUM

As a rule, the electron spectrum of real conductors is far from the model we have considered above. The nonspherical and nonquadratic character of the spectrum, and also the fact that the Fermi surface is multiply connected and open orbits exist, lead to a change in the dynamics of an individual electron and, because of this, to a substantial change in the spectrum of the collective electromagnetic excitations. Calculation of the conductivity tensor for a fairly complicated model of the electron spectrum is possible only in individual cases, and is carried out by approximating the real spectrum by a function such as will make it possible to obtain analytical expressions for σ_{ik}. In conditions when it does not appear possible to calculate the conductivity tensor, the use of the conservation laws to analyze the different resonance effects in classically-strong and quantizing fields in metals with an anisotropic spectrum may turn out to be useful to a still greater degree than in the previous cases.

To what qualitative changes in the electromagnetic-excitation spectrum does anisotropy of the electron spectrum lead? First, because of the change in the symmetry of the ground state, even for $\mathbf{q} \parallel \mathbf{H}$ the selection rules do not forbid electron transitions with $\Delta n \neq 0$ for longitudinal waves or transitions with $\Delta n \neq \pm 1$ for circularly polarized waves. Therefore, in metals with a complicated Fermi surface, electromagnetic excitations shaped by additional singularities of the conductivity tensor can exist. Secondly, new branches can appear as a result of the multi-component character of the system, i.e., because of the existence of several closed parts of the Fermi surface, inequivalently located with respect to the magnetic field. It is also necessary to keep in mind that, in real metals, the singularities of the conductivity tensor at the collisionless-damping thresholds can be stronger than in a model with a quadratic spectrum. The strengthening of a singularity of the conductivity leads to a substantial change in the pre-threshold spectrum of the different excitations. Thus, near a Doppler-shifted cyclotron resonance, helicon and Alfven waves go over into a doppleron. Interesting resonance effects can exist in metals with open Fermi surfaces. For example, motion of electrons in the direction perpendicular to the magnetic-field direction and the direction in which the Fermi surface is open (in p-space) leads to a shift of the cyclotron frequency because of the Doppler effect, and, because of this, to a radical rearrangement of the spectrum of the cyclotron waves.

A. Electromagnetic waves in conductors with an anisotropic quadratic spectrum

Many characteristic features of the spectrum of electromagnetic waves in metals with an anisotropic quadratic spectrum are conveniently traced using the example of bismuth. In this subsection we shall not consider the electromagnetic excitations which already exist in metals with an isotropic electron spectrum. The effect of the anisotropy of the electron spectrum of bismuth on the spectrum of the electromagnetic excitations that exist in the isotropic model has been considered in detail in the reviews[1,4].

The Fermi surface of bismuth is well-known (cf., e.g., [57]). It consists of one hole ellipsoid oriented along the trigonal axis and three strongly anisotropic electron ellipsoids[2)], positioned in the plane perpendicular to the C_3-axis. The hole and electron ellipsoids are positioned at the Brillouin-zone boundaries, the longest axis of the electron ellipsoids being inclined at an angle ~6° to the basal plane. The contribution to the conductivity tensor from one ellipsoid is equal to[59]

$$\sigma_{ik}^{j} = \frac{ie^2 n_j}{m\omega}\delta_{ik} + \frac{ie^2}{\omega}\sum_{\alpha,\beta}\frac{(f_\beta - f_\alpha)\langle\alpha|V_i|\beta\rangle\langle\alpha|V_k|\beta\rangle^*}{\varepsilon_\beta - \varepsilon_\alpha - \hbar\omega - i\delta}, \qquad (5.1)$$

where j is the valley index, α_{ik} is the dimensionless tensor of the inverse effective masses,

[2)] The energy spectrum and the shape of the Fermi surface of bismuth are described in more detail by the model of Cohen.[58]

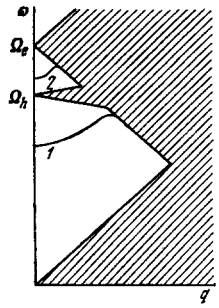

FIG. 6. Spectrum of the longitudinal (1) and transverse (2) waves in bismuth ($\mathbf{q} \parallel \mathbf{H} \parallel C_3$). (The dispersion curves of the Alfven wave, the fast magnetosonic wave and the Pines-Schrieffer wave are not shown in the figure.)

$$v_i = \frac{\alpha_{ik}}{m}\left(p_k + \frac{e}{c}A_k\right),$$

and $|\alpha\rangle$ is a solution of the Schrödinger equation for a particle with an anisotropic quadratic dispersion law.[60]

First we shall consider electromagnetic excitations in nonquantizing magnetic fields,[61] propagating along directions defined by the crystal symmetry: $\mathbf{q} \parallel \mathbf{H} \parallel C_3$ or $\mathbf{q} \parallel \mathbf{H} \parallel C_2$. In the first case it follows from the symmetry that the nonzero components of σ_{ik} have the form[62]

$$\sigma_{xx} = \sigma_{yy} = \frac{r_j}{2}(\sigma^j_{xx} + \sigma^j_{yy}),$$
$$\sigma_{xy} = \frac{r_j}{2}(\sigma^j_{xy} - \sigma^j_{yx}), \qquad (5.2)$$

where r_j is the number of equivalent valleys. If $\mathbf{q} \parallel \mathbf{H} \parallel C_2$, the components σ_{xx}, σ_{xy}, $\sigma_{yy} \neq \sigma_{xx}$ and σ_{zz} are nonzero, and $\sigma_{ik} = r_j \sigma^j_{ik}$.

Suppose that a circularly polarized wave propagates along the C_3-axis. Then, as follows from the expressions (5.1) and (5.2), for $q \to 0$ electron transitions with $\Delta n = \pm 1$ are allowed for each circular polarization, as are hole transitions with $\Delta n = -1$ for left circular polarization and $\Delta n = 1$ for right circular polarization. The simultaneous existence of electron transitions with $\Delta n = 1$ and $\Delta n = -1$ for each polarization is connected with the fact that the electron parts of the Fermi surface are nonspherical. The collisionless-damping regimes in bismuth, depicted in Fig. 6, determine the boundaries of existence of the new right-polarized excitation associated with the electron and hole transitions with $\Delta n = 1$. The dispersion equation for the transverse waves for $q \to 0$ has the form

$$\frac{\alpha_1^e + \alpha_2^e}{2}\frac{\omega_p^2}{\Omega_e^2 - \omega^2} \pm \frac{\omega_p^2}{\omega\Omega}\frac{\Omega_e^2}{\Omega_e^2 - \omega^2} - \frac{\alpha_1^h \omega_p^2}{\omega(\omega \pm \Omega_h)} = \frac{c^2 q^2}{\omega^2}; \qquad (5.3)$$

here $\Omega_e = \Omega\sqrt{\alpha_1^e \alpha_2^e}$, $\Omega_h = \alpha^h \Omega$, $\alpha_{xx} = \alpha_1$, $\alpha_{yy} = \alpha_2$, $\alpha_{zz} = \alpha_3$ and $\alpha_{xy} = \alpha_4$. It follows from Eq. (5.3) that, along C_3 in the range $\Omega_h < \omega < \Omega_e$, there exists a right-polarized electromagnetic excitation having the spectrum[62]

$$\omega = \omega(0) + \frac{(\omega(0) - \Omega_h)(\Omega_e^2 - \omega^2(0))}{(\alpha_1^e + \alpha_2^e + 2\alpha_1^h)\omega_p^2 \omega^2(0)} c^2 q^2, \quad \omega(0) = \Omega_h\left[1 + \frac{2(\alpha_1^e \alpha_2^e - (\alpha_1^h)^2}{\alpha_1^h(\alpha_1^e + \alpha_2^e + 2\alpha_1^h)}\right]. \qquad (5.4)$$

In the region $\omega < \Omega_{e,h}$, (5.3) gives the spectrum of the Alfven and fast magnetosonic waves. The imaginary part in (5.4) is of the order of the collision frequency. The solution (5.4), as already noted, arises only because of the fact that, together with the hole transitions with $\Delta n = 1$, electron transitions with $\Delta n = 1$ are also allowed.

In other semimetals (antimony, arsenic), where the hole parts of the Fermi surface do not lie on the C_3-axis and, consequently, are not surfaces of revolution, electron and hole transitions with $\Delta n = \pm 1$ are allowed and there exists both a right-polarized and a left-polarized excitation of the type (5.4).

In the propagation of longitudinal waves along the C_3-axis in bismuth, because of the declination of one of the principal axes of the electron ellipsoids from the basal plane, besides the transitions with $\Delta n = 0$ there arise additional resonances with $\Delta n = \pm 1$, which form the spectrum of a new longitudinal excitation. The solution of the dispersion equation

$$\varepsilon_{zz}^0 - \frac{\omega_p^2}{\omega^2}(\alpha_3^e + \alpha_3^h + r^2 q^2) + \frac{(\alpha_4^e)^2 \omega_p^2}{\alpha_2^e(\Omega_e^2 - \omega^2)} = 0, \qquad (5.5)$$

where ε_{zz}^0 is the dielectric permittivity of the lattice,

$$r^2 = \frac{3}{5}\left(\frac{v_{Fe}^2 + v_{Fh}^2}{\omega^2} - \frac{1}{3}\frac{(\alpha_4^e)^2 v_{Fe}}{\alpha_2^e \Omega_e^2}\right),$$

has, for $q \to 0$, the form

$$\omega^2 = \omega^2(0)(1 + \rho^2 q^2) \qquad (5.6)$$

(cf. Fig. 6). Here,

$$\omega^2(0) = \Omega_e^2(1 - \gamma_e), \quad \rho^2 = \frac{3v_{Fe}^2 \gamma_e}{5\omega^2(0)}\left(\frac{\Omega_e^2}{\omega^2(0)} - \frac{1}{3}\gamma_e\right), \quad \gamma_e = \frac{(\alpha_4^e)^2}{\alpha_2^e(\alpha_3^e + \alpha_3^h)}.$$

In the isotropic model, in the propagation of a wave at an angle to the magnetic field, transitions with arbitrary Δn are allowed. But their contribution to the conductivity is proportional to some power of q and, therefore, solutions analogous to (5.4) and (5.6) do not arise.

If the magnetic field is directed along a two-fold axis, then two inequivalent electron groups and one hole group of carriers exist in bismuth. In this case the principal axis of one of the electron ellipsoids and of the hole ellipsoid is parallel to **H**. The principal axes of the other two electron ellipsoids do not coincide with the magnetic-field direction. Thus, the electron system is a two-component system and is characterized by two cyclotron frequencies Ω_{e1} and Ω_{e2}. It is not difficult to convince oneself that, for $qv_F \ll |\omega - \Omega_j|$ in the range $\Omega_{e1} < \omega < \Omega_{e2}$, even in the isotropic model, in a two-component plasma with the same types of carriers there should exist a transverse electromagnetic excitation for which the polarization vector rotates in the same direction as the electrons. It is not surprising, therefore, that in bismuth, with **H** parallel to the C_2-axis, there exists such an electromagnetic wave. Its spectrum can be found by writing the dispersion equation for $qv_F \ll |\omega - \Omega_j|$:

$$\left[\left(\varepsilon_{xx} - \frac{c^2 q^2}{\omega^2}\cos^2\vartheta\right)\left(\varepsilon_{yy} - \frac{c^2 q^2}{\omega^2}\right) - \varepsilon_{xy}\varepsilon_{yx}\right] = 0(q^4), \qquad (5.7)$$

where ϑ is the angle between $\mathbf{H} \parallel C_2$ and the vector $\mathbf{q}$, which lies in the (x, z)-plane. The expressions for the tensor components ε_{ij} and the dependence $\omega(q)$ are extremely cumbersome. Therefore, following the paper[63], we give only the numerical values of the coefficients in the function $\omega(q)$. For $\mathbf{q} \parallel \mathbf{H} \parallel C_2$, the solution of (5.7) in the range $\Omega_{e1} < \omega < \Omega_{e2}$ has the form

$$\omega = 5.35\Omega_h \left\{1 + \left[0.34 + 0.27\left(\frac{500}{H}\right)^2\right] 10^{-7} q^2\right\}. \quad (5.8)$$

If $\mathbf{q} \perp \mathbf{H} \parallel C_2$, $\mathbf{q} \parallel C_3$, then

$$\omega = 5.35\Omega_h \left\{1 + \left[0.25 + 0.37\left(\frac{500}{H}\right)^2\right] 10^{-7} q^2\right\}. \quad (5.9)$$

The spatial dispersion of the conductivity tensor has been taken into account in these expressions.

The excitations (5.8) and (5.9) have been observed through the oscillations of the surface impedance of plates of bismuth.[63] The dependences $\partial R/\partial H$ and $\partial X/\partial H$ (the surface impedance $Z = R + iX$) are given in Figs. 7 and 8. The experimental conditions are indicated in the captions to the figures. The dependence $\omega(q)$ found experimentally practically coincides with (5.8) and (5.9), if we assume that for $\mathbf{q} \parallel \mathbf{H} \parallel C_2$ Rayleigh resonances are observed ($n\lambda = d$ where d is the thickness of the plate and λ is the wavelength) while for $\mathbf{H} \perp \mathbf{q} \parallel C_3$ Fabry–Perot resonances are observed ($n\lambda/2 = d$). The limiting frequency $\omega(0)$ of the excitations (5.8) and (5.9) was also determined in the paper[64], in which the transmissivity of bismuth was studied in the infrared region. That the frequency $\omega(0)$ exists for $\mathbf{q} \perp \mathbf{H}$ had been pointed out in [65], in which this phenomenon was called a dielectric anomaly.

A longitudinal wave whose origin is explained by the anisotropy of the electron spectrum can also propagate along the C_2-direction. In fact, in a magnetic field directed along the C_2-axis, for one group of electrons and for the holes, transitions with $\Delta n = 0$ are allowed. For the other two electron ellipsoids, for which none of the principal axes coincides with the direction of H, transitions with $\Delta n = \pm 1$, giving rise to an additional singularity, analogous to (5.5), in the component ε_{zz}, are allowed. This leads to the existence of a solution of the equation $\varepsilon_{zz} = 0$ in the range $0 < \omega < \Omega_{e1}$.

From the point of view of observing quantum waves, semimetals are the most promising. This is explained by the happy conjunction of the parameters determining

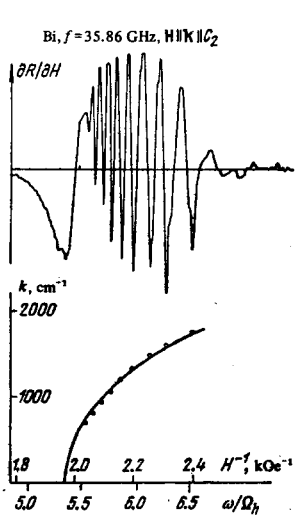

FIG. 7. Rayleigh resonances and the dependence $k(\omega/\Omega_h)$ obtained for a bismuth plate of thickness 0.47 mm at temperature $T \approx 1.5$ K. (The points are experimental; the curve of $k(\omega/\Omega_h)$ is constructed from formula (5.8).)

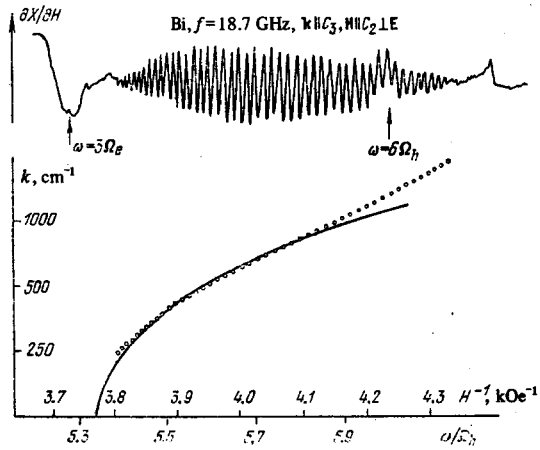

FIG. 8. Fabry-Perot resonances and the dependence $k(\omega/\Omega_h)$, obtained for a bismuth plate of thickness 2 mm at temperature $T \approx 0.6$ K. (The points are experimental and the curve of $k(\omega/\Omega_h)$ is constructed from formula (5.9).)

the spectrum and damping of the excitations in the semimetals. The low carrier concentrations and small effective masses in semimetals appear in conjunction with a long carrier lifetime. In addition, the strong anisotropy of the electron spectrum leads to the existence of quantum waves with longitudinal and transverse polarization in all windows.

Longitudinal and transverse quantum waves associated with transitions $\Delta n = 0$ in semimetals were first studied in the papers[33,62]. Here, following[62], we consider transverse quantum waves. In bismuth and antimony, longitudinal and transverse waves propagate independently along the C_3-axis. As already noted, a contribution to the conductivity tensor $\sigma_\pm$ for circularly polarized excitations is given not only by transitions with $\Delta n = \pm 1$ but also by those with $\Delta n = 0$. This leads to the appearance of circularly polarized waves in the windows depicted in Fig. 1. According to (3.20) and (5.1), the dispersion equation for these has the form[62]

$$1 - \frac{\omega}{\omega_r} - \frac{u^2}{v_\alpha^2} = \sum_{e,h} \mu G(u), \quad (5.10)$$

where $u = \omega/q$, $\omega_r = cH/4\pi n_0 e\rho^2 \sim \Omega v_\alpha^2/v_F^2$ (at frequencies $\omega > \omega_r$, spatial dispersion becomes important in the spectrum of the Alfven and fast magnetosonic waves[66]),

$$\rho^2 = \rho_e^2 - \rho_h^2, \quad \rho_i^2 = \left(\frac{c}{eH}\right)^2 \frac{m_0 \varepsilon_F^i}{\alpha_{1i}\alpha_{2i}^3}\left(\alpha_{4i}^2 - \frac{2}{5}\alpha_{2i}\alpha_{3i}\right), \quad (5.11)$$

v_α is the velocity of the Alfven wave in the semimetal, and the coefficient $\mu = 3\pi n_0 \varepsilon_F \alpha_4^2/\alpha_2^2 H^2$ is equal in order of magnitude to the ratio of the Fermi-energy density to the magnetic-energy density. The function $G(u)$ is equal to

$$G(u) = \sum_{n=0}^{n_F} \chi(n)\left[\left(1 - \frac{u^2}{v_n^2}\right)^{-1} - 1\right], \quad (5.12)$$

$$\chi(n) = \left(\frac{n}{n_F + \Delta}\right)^2 [(n_F + \Delta)(n_F + \Delta - n)]^{-1/2}, \quad (5.13)$$

where Δ is the noninteger part of the ratio $\varepsilon_F/\hbar\Omega$. Eq. (5.10) is valid under the condition $|u - v_n| \gg \hbar q/2m$, which allows us to expand the logarithms in the tensor

component ε_{xx}. In the opposite case, when the solution $u_n(\omega)$ lies near v_n, the singularities in the right-hand side of (5.10) are logarithmic.

The left-hand side of Eq. (5.10) vanishes at the spectrum of the Alfven or fast magnetosonic wave[3)]. For $v_\alpha < v_F$, because of the smallness of the coefficient μ, solutions of Eq. (5.10) that correspond to quantum waves exist only near the classical solutions, in the windows nearest to the one in which the left-hand side of (5.10) is equal to zero. Thus, quantum waves appear in the neighboring windows as satellites of the Alfven and fast magnetosonic waves. If $v_\alpha < v_F$, the left-hand side of (5.10) is large in all the windows and quantum waves are absent. We note that, in bismuth, the inequality $v_\alpha > v_F$ is fulfilled even in nonquantizing fields. Therefore, the conditions for observing transverse quantum waves associated with $\Delta n = 0$ transitions are unfavorable in bismuth. The most favorable conditions for observing the quantum waves under consideration are realized in antimony, where, because of the relatively high carrier concentration, the requirement $v_\alpha < v_F$ is fulfilled in quantizing magnetic fields.

We shall establish the criterion for the existence of transverse quantum waves. For quantum waves to exist it is necessary that the magnitude of the right-hand side of Eq. (5.10) at a singular point for finite ν and T be greater than the left-hand side of the equation. Moreover, the quantum waves will be damped only as a result of collisions, if the corresponding dispersion curve is distant from the boundary of the window by an amount greater than the impurity and thermal smearing-out of the boundary.

If the inequality $|u - v_n| \gg \hbar q/2m$ is not fulfilled and the velocity $u_n(\omega)$ of the quantum wave is close to $v_n \sim v_\alpha$, then these two conditions coincide and have the form

$$\left|\ln\frac{\nu}{qv_n}\right| \gg \left(1 \mp \frac{\omega}{\omega_r} - \frac{u_n^2}{v_\alpha^2}\right)\mu^{-1}, \qquad \left|\ln\frac{T}{mv_n^2}\right| \gg \left(1 \mp \frac{\omega}{\omega_r} - \frac{u_n^2}{v_\alpha^2}\right)\mu^{-1}. \tag{5.14}$$

The conditions for the existence of quantum waves in the windows adjoining the window where the Alfven wave is located are less stringent than (5.14). As follows from Eq. (5.10), the velocity difference $u_n(\omega) - v_n$ in this case is of the order of $\alpha\hbar\Omega/mv_n$, where $\alpha \lesssim 1$. (The exact value of this coefficient can be found by solving Eq. (5.10) numerically.) By requiring that the difference $u_n(\omega) - v_n$ be greater than the thermal and impurity broadening of the damping boundaries, we obtain

$$T \ll \alpha\hbar\Omega, \qquad \nu \ll \alpha\omega\frac{v_{nF}^2}{v_n^2}. \tag{5.15}$$

We note that these conditions are sufficient for observation of giant quantum oscillations in the absorption of the Alfven and fast magnetosonic waves (cf. (4.25)).

[3)]The nonresonance terms in the right-hand side lead to a renormalization of the velocity of the magnetoplasma waves. Below we shall assume that such a renormalization has been carried out and that only resonance terms remain in the right-hand side.

It follows from (5.15) that in quantizing magnetic fields corresponding to $\mu \sim 1-10^{-1}$ and $v_\alpha < v_F$, for $T \lesssim 1$ K and $\omega \sim 10^{11}-10^{12}$ sec^{-1}, weakly-damped transverse quantum waves associated with $\Delta n = 0$ transitions can propagate in antimony in a few windows nearest to the one in which the Alfven wave is situated.

B. Electromagnetic waves in metals with a complicated Fermi surface

1) We now consider the spectrum of electromagnetic excitations in metals with a more complicated Fermi surface. The conductivity tensor in classically-strong magnetic fields in metals with an arbitrary electron dispersion law has the form[11]

$$\sigma_{ik}(\omega, \mathbf{q}, \mathbf{H}) = \frac{ie^2}{2\pi^2\hbar^3}\int dp_z\,|m_c|\sum_{\Delta n=-\infty}^{+\infty}\frac{V_{\Delta n,i}V^*_{\Delta n,k}}{\omega - \tilde{\mathbf{v}}\mathbf{q} \div \Delta n\Omega + i\nu}, \tag{5.16}$$

where $m_c(p_z) = (1/2\pi)\partial S/\partial\varepsilon$ is the cyclotron mass, $\Omega = eH/m_c c$, $S(\varepsilon, p_z)$ is the area of the section of a constant-energy surface cut by the plane $p_z = \text{const}$, the magnetic field is directed along the z-axis,

$$V_{\Delta n,i} = \frac{1}{2\pi}\int_0^{2\pi} v_i(\tau)\exp\left\{-\frac{i}{\Omega}\int_0^{\tau}\{q[\mathbf{v}(\tau') - \tilde{\mathbf{v}}] + \Delta n\Omega\}\,d\tau'\right\}d\tau, \tag{5.17}$$

$$\tilde{\mathbf{v}} = \frac{1}{2\pi}\int_0^{2\pi}\mathbf{v}(\tau)\,d\tau, \qquad \tilde{v}_z = -\frac{1}{2\pi m_c}\frac{\partial S}{\partial p_z}, \tag{5.18}$$

$v_i(\tau)$ is a component of the electron velocity at the Fermi surface and $\tilde{\mathbf{v}}$ is the value of the velocity averaged over a cyclotron period. We note that the summation over harmonics in (5.16) corresponds in the quantum case to summation over transitions Δn. Which Δn are allowed now?

We shall consider a circularly polarized wave propagating along the magnetic field, which is directed along a symmetry axis of high order. Suppose that the electron orbits on a certain part of the multiply-connected Fermi surface have an m-th-order symmetry axis. In this case, [67] the selection rules for $V^{\pm}_{\Delta n} = V_{\Delta nx} \pm V_{\Delta ny}$ can be found from (5.17) by expanding the function $v_i(\tau)$ and the exponent in a Fourier series. It is not difficult to see that the function $V^{\pm}_{\Delta n}$ is not equal to zero if

$$\Delta n = ms \pm 1, \qquad s = 0, \pm 1, \pm 2, \ldots \tag{5.19}$$

For hole orbits the upper sign in the selection rules (5.19) corresponds to right, and the lower sign to left circular polarization. As we already know, $\Delta n = \pm 1$ corresponds to an axially symmetric Fermi surface. The selection rules for an arbitrary wave in the same geometry have the form

$$\Delta n = ms, \qquad s = 0, \pm 1, \pm 2, \ldots \tag{5.20}$$

For an arbitrary orientation of the vectors $\mathbf{q}$ and $\mathbf{H}$ with respect to a symmetry axis of the Fermi surface, transitions with any Δn are allowed.

The denominator in the integrand of (5.16), for $\nu \to 0$, vanishes on the straight lines

$$\omega = \Delta n\cdot\Omega(p_z) \pm \tilde{v}_z(p_z)q_z. \tag{5.21}$$

This is the condition for resonance absorption of the wave by electrons with a specific p_z. Clearly, the col-

lisionless-damping boundary can be found as the envelope curve of the family of straight lines (5.21). In other words, the damping boundaries are obtained from Eq. (5.21) and the equation

$$\Delta n \frac{\partial \Omega(p_z)}{\partial p_z} = \pm q_z \frac{\partial v_z}{\partial p_z} \tag{5.22}$$

after elimination of the variable p_z. Consequently, to construct the collisionless-damping boundaries it is necessary to find first the cyclotron frequency and the orbit-averaged velocity as a function of p_z. If the family of straight lines (5.21) does not have an envelope, the boundaries of the collisionless-damping regimes are determined by the expression (5.21) with the extremal values of the cyclotron frequency and longitudinal electron velocity. Thus, the shape of the boundaries turns out to be intimately connected with the geometry of the Fermi surface.

On the boundaries, determined by Eqs. (5.21) and (5.22), of the collisionless-damping regimes, the conductivity has singularities which form a spectrum of new electromagnetic excitations. In particular, for this reason, near the boundary of the Doppler-shifted cyclotron resonance there appear the modes first considered in [68,69] and afterwards called dopplerons.[70] The character of the singularity depends on the geometry of the Fermi surface.

With the aid of the expression (5.16) it is possible to carry out a general analysis of the singularities of the conductivity tensor on the collisionless-damping boundaries. Here, for simplicity, we shall confine ourselves to treating two cases: $\omega \to 0$ and $q \to 0$. The hierarchy of singularities of the conductivity for $\omega \to 0$ was studied in [71] for different models of the Fermi surface. The authors of this paper started from the conductivity expression[72]

$$\sigma_\pm(q, H) = \frac{iec}{4\pi^3 H\hbar^3} \int dp_z \frac{S(p_z)}{1 - u(p_z) q \pm i\eta}, \tag{5.23}$$

which is obtained from the expression (5.16) for $\omega \ll \Omega$, ν and $\Delta n = 1$. Here,

$$u(p_z) = \frac{c}{2\pi eH} \frac{\partial S}{\partial p_z} = -\frac{\tilde{v}_z(p_z)}{\Omega(p_z)} \tag{5.24}$$

is the average displacement of electrons in the direction of the magnetic field in a cyclotron period and $\eta = \nu/\Omega$.

The type of singularity of the conductivity is determined by the behavior of the function $S(p_z)$ near the point p_0 at which the displacement $u(p_z)$ of the electrons in a cyclotron period is extremal. It is clear that the singularity will be stronger in the case when the numerator of the integrand in (5.23)—the area of a section of the Fermi surface—does not vanish at the point p_0. By expanding the area S and the derivative $\partial S/\partial p_z$ about p_0, we can find, after calculations in (5.23), that[71]

$$\sigma_\pm \sim [1 - u(p_0) q \pm i\eta]^{-(n-1)/n}, \tag{5.25}$$

if $S(p_0) \neq 0$, $\partial S(p_0)/\partial p_z \neq 0$ and $\partial^n S(p_0)/\partial p_z^n = 0$ but $\partial^{n+1} S(p_0)/\partial p_z^{n+1} \neq 0$, $n \geq 2$. For example, for an electron spectrum with a Fermi surface of the pinched-cylinder type:

$$\varepsilon = \frac{p_\perp^2}{2m} + \varepsilon_0 \sin^2 \frac{\pi p_z}{2k}, \tag{5.26}$$

if the magnetic field is directed along the axis of the cylinder, $n = 2$ (ε_0 is the width of the energy band and $2k$ the size of the Brillouin zone). Consequently, $\sigma_\pm$ has a square-root singularity. For the parabolic model of Chambers and Skobov[73]:

$$\varepsilon = \frac{p_\perp^2}{2m} + v|p_z| \tag{5.27}$$

$n = \infty$ and the conductivity has a first-order pole. If the section of the Fermi surface vanishes at the point p_0 ($S(p_0) = 0$), while $\partial S(p_0)/\partial p_z \neq 0$, $\partial^n S(p_0)/\partial p_z = 0$, $\partial^{n+1} S(p_0)/\partial p_z^{n+1} \neq 0$ and $n > 2$, the conductivity has singularities of the form[71]

$$\sigma_\pm \sim [1 - u(p_0) q \pm i\eta]^{-(n-2)/n}. \tag{5.28}$$

For $n = 2$ (elliptical limiting point) the singularity of $\sigma_\pm$ is of the type $x \ln x$. It can be seen from the expressions given that the singularity is stronger if the area of the section at the point where the displacement in a cyclotron period is extremal is not equal to zero. This was first pointed out by McGroddy, Stanford and Stern[68] and Overhauser and Rodriguez, [69] who studied the behavior of the helicon spectrum near the boundary of the Doppler-shifted cyclotron resonance in a model for the electron spectrum of a metal in a state with a periodic spin-density distribution.[74] Because of the strengthening of the singularity of the conductivity, the helicon spectrum near the threshold was altered: the helicon went over into a doppleron.

A doppleron exists as a weakly damped excitation in the case when its dispersion curve is at a sufficient distance from the collisionless-damping boundary. This means that dopplerons are well-defined in metals in which the geometry of the Fermi surface leads to a sufficiently strong singularity of the nonlocal conductivity. In fact, if the maximum velocity (displacement during a cyclotron period) is reached at an elliptical limiting point, then, for a helicon or for Alfven waves, the spectrum is cut off at the damping threshold. If the conductivity singularity is logarithmic, then, as follows from the dispersion equation, the dispersion curve lies at an exponentially small distance. A power-law singularity of the nonlocal conductivity gives the greatest distance from the threshold.

2) In recent years, dopplerons in metals having a complicated Fermi surface have been investigated in the work of Konstantinov, Skobov, Fisher, and others. To calculate the conductivity tensor, sufficiently simple models of the Fermi surface have been used; these, on the one hand, have made it possible to find analytical expressions for $\sigma_\pm$, and, on the other, have given a qualitatively correct description of the Fermi surface as known from other experimental and theoretical work. A survey of work on dopplerons is given by Skobov in the Appendix to the monograph[9]. In the present review, without going into the details of the experiments and theory, we shall discuss only certain characteristic features of the doppleron solutions. We shall be interested principally in the origin of dopplerons and

their relationship to the geometry of the Fermi surface, and also in the place of dopplerons in a unified system of electromagnetic excitations.

The doppleron in cadmium[75,76] is formed by electrons from the third Brillouin zone; the Fermi surface of these electrons resembles a lens[77] and the resonance for $\mathbf{q} \parallel \mathbf{H} \parallel C_6$ is associated with the electrons at the limiting point. In addition, in cadmium there exists a hole doppleron due to the resonance at the hole orbits located near the maximum (central) section of the monster in the second Brillouin zone. The functions $S_e(p_z)$ and $S_h(p_z)$ and their derivatives, found in [78], were approximated in[75] by simple analytical expressions leading to a logarithmic singularity of the electron and hole conductivity. The parameters of the spectrum of the dopplerons discovered experimentally in[75] agree well with the proposed model.

In copper the doppleron spectrum is highly distinctive.[79] This is explained by the fact that, on moving along p_z with **H** directed, e.g., along the two-fold axis, we first encounter hole orbits, then electron orbits, and arrive at open trajectories. By letting **H** deviate from the two-fold axis by an angle greater than 2°, it is possible to get rid of the open trajectories. The hole parts of the Fermi surface do not lead to a singularity of the nonlocal conductivity, since, in the model taken for the Fermi surface in [79], $u(p_z) \sim \partial S/\partial p_z$ changes monotonically from $-\infty$ to $+\infty$. This means that collisionless damping exists for all q and there are no thresholds.

The crossing from hole orbits to electron orbits is accompanied, at a certain value of p_z, by a finite discontinuity in the area $S(p_z)$ and by the divergence of the derivative $\partial S/\partial p_z$ to $+\infty$. The singularity is connected with the fact that the limiting orbit passes through a saddle point. These functions behave analogously when we go from closed electron orbits to open ones. Consequently, at a certain value of p_z within the range corresponding to the electron orbits, the derivative $\partial S/\partial p_z$ has a minimum, and this leads to collisionless damping at low q, up to a certain $q_{max} = 2\pi eH/c(\partial S/\partial p_z)_{min}$, and to its absence for $q > q_{max}$. At the threshold the electronic conductivity in the model used in [79] has a root singularity and, therefore, a doppleron exists here. When **H** is directed exactly along the twofold axis, because of the open orbits the helicon is strongly damped.[80] Therefore, the doppleron spectrum in copper[79] in the long-wavelength region does not go over into a helicon spectrum. If the direction of the magnetic field is such that open trajectories are absent, both excitations exist. The graphs of the functions $S(p_z)$ and $\partial S/\partial p_z$ for other directions, constructed by Powell and given in [81], make it possible to find the thresholds and analyze the possibility of the existence of dopplerons propagating along other crystallographic directions.

All the models considered up to now have possessed axial symmetry, which, in a number of cases, did not correspond to the actual symmetry of the Fermi surface. The defect of these models is that they do not take into account all the electron transitions allowed by the selection rules (cf. (5.19), (5.20)) and, consequently, do not describe the electromagnetic excitations associated with the additional resonances. In a paper[82] devoted to the study of multiple dopplerons in aluminum, a Fermi-surface model with a fourth-order symmetry axis was used and gave qualitatively correct agreement with the result of a numerical calculation of the functions $S(p_z)$, $\partial S/\partial p_z$ and $\Omega(p_z)$ found by Larsen and Greisen.[67] The Fermi surface in aluminum, as is well-known, consists of a large hole surface in the second Brillouin zone and a small electron surface in the third zone. Since the electron concentration is small (less than 3% of the hole concentration), the electron contribution to the conductivity was not taken into account in[82]. In accordance with the selection rules (5.19), right-polarized dopplerons associated with resonances $\Delta n = 1, 5, 9$ and left-polarized dopplerons formed by transitions with $\Delta n = 3, 7$ should propagate in the [100] direction in aluminum. The theory of multiple dopplerons in aluminum, developed in [82], gives a qualitatively correct description of the experimental results. Of course, besides the dopplerons, in aluminum there exists the helicon studied in detail by Larsen and Greisen.[67] The collisionless-damping regimes and the schematic form of the dispersion curves of the helicon, dopplerons and anisotropons in aluminum are shown in Fig. 9. The damping thresholds are constructed from formulas (5.21) and (5.22) using the functions $\Omega(p_z)$ and $\bar{v}_z(p_z)$ from [67]. Dopplerons in indium, in which the Fermi surface is similar to that of aluminum, were discovered in [83]. We note also that Konstantinov and Skobov[84,85] predicted doppleron solutions of the Maxwell equations, with **q** almost perpendicular to **H**, for alkali metals in which the Fermi surface is practically isotropic. The appearance of the solution is due to the strengthening of the conductivity singularity in this geometry.

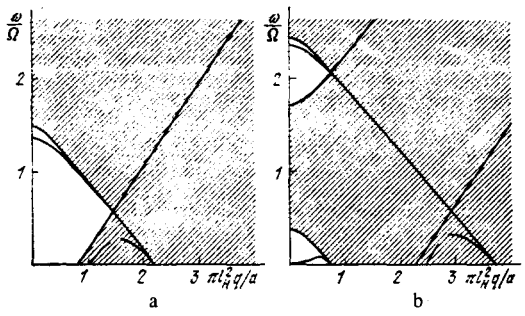

FIG. 9. Spectrum and regimes of collisionless damping of left-polarized (a) and right-polarized (b) waves in aluminum for $\mathbf{q} \parallel \mathbf{H} \parallel C_4$. (The damping boundaries in Fig. 9a correspond to resonances with $\Delta n = 3$ and $\Delta n = -1$, and in Fig. 9b to resonances with $\Delta n = 1$, 5 and $\Delta n = -3$. The dispersion curves of the helicon, dopplerons and anisotropons are depicted schematically.)

The singularities of the dielectric permittivity not only shape the spectrum of the characteristic electromagnetic waves in a metal, but are also intimately connected with the phenomena of trajectory penetration of an electromagnetic field into a metal.[45] The connection between natural modes whose spectrum lies near

resonances and the anomalous-penetration effects is most clearly manifested in the example of the doppleron. Since the doppleron is positioned near to the boundary of the Doppler-shifted cyclotron resonance, the wavelength of the doppleron differs insignificantly from the maximum displacement of electrons along the field during a cyclotron period, which determines the period of the Gantmakher-Kaner radio-frequency size effect. Therefore, the surface-impedance oscillations associated with resonance excitation of a doppleron and with the size effect have similar periods in the magnetic field. The magnitude of both types of oscillation of the impedance depends on the geometry of the Fermi surface. This dependence has been discussed in detail in the already mentioned papers[75, 79, 82–85]. The collisionless-damping thresholds shown below in Fig. 12 make it possible to find the period of the size effect for different Δn at a finite frequency.

Dopplerons exist in a region where time dispersion is unimportant. Therefore, in theoretical papers in which dopplerons have been studied, it has been assumed that $\omega \ll \Omega$ and that the experiment is performed at radio frequencies. Electronic transitions that are absent in a model with an isotropic spectrum and are allowed by the selection rules (5.19) and (5.20) give rise to the existence of other electromagnetic waves in metals. In order to demonstrate this, we shall consider the region where time dispersion of the conductivity is important and spatial dispersion is absent. In (5.16) we put $\omega \neq 0$ but $q = 0$. Then,

$$\sigma_{\pm}(\omega, H) = \sigma_{xx} \pm i\sigma_{yx} = \frac{ie^2}{4\pi^2\hbar^3} \int dp_z |m_c| \sum_{\Delta n=-\infty}^{+\infty} \frac{V_{\Delta n}^{+}(V_{\Delta n}^{+} \mp V_{\Delta n}^{-})}{\omega - \Delta n\Omega(p_z) - i\nu}. \tag{5.29}$$

In the isotropic model, for $\mathbf{q} \parallel \mathbf{H}$ and $q \to 0$, the conductivity σ_+ as a function of frequency has a single singularity of the form $(\omega - \Omega)^{-1}$. In an anisotropic model the denominator of (5.29) vanishes, for $\nu \to 0$, at frequencies $\omega - \Delta n\Omega(p_z) = 0$. The integration over p_z weakens this singularity. We shall be interested in the region $\Delta n\Omega_{min} < \omega < \Delta n\Omega_{max}$, in which the collisionless damping is equal to zero and undamped circularly polarized excitations can exist. It is obvious that frequency ranges in which damping is absent exist only for sufficiently small values of Δn. The behavior of the function $\sigma_+(\omega)$ as $\omega \to \Delta n\Omega_{extr}$ can be found analogously to (5.25) and (5.28). If at the extremal point p_0 the function $\Omega(p_z)$ has the form $\Omega(p_z) = \Omega_{extr} + \alpha(p - p_0)^{2n}$ and the numerator of (5.29) does not vanish, then the conductivity has a singularity of the form

$$\sigma_{\pm}(\omega) \sim (\omega - \Delta n\Omega_{extr})^{-\frac{(2n-1)}{2n}}. \tag{5.30}$$

It is not difficult to convince oneself that the singularities of σ_+ have opposite signs in the windows near $\Delta n\Omega_{min}$ and $\Delta n\Omega_{max}$. This means that a solution of Eq. (4.6) exists in the interval $\Delta n\Omega_{min} < \omega < \Delta n\Omega_{max}$. It is natural to call excitations of this type, associated with the anisotropy of the electron spectrum, anisotropons. In an analogous way, we can convince ourselves that in the frequency ranges $\Delta n\Omega_{min} < \omega < \Delta n\Omega_{max}$ with Δn from (5.20), longitudinal excitations should exist. It follows from what has been said that the existence of transverse and longitudinal anisotropons is essentially connected with the fact that in metals with an anisotropic spectrum the electrons move in noncircular cyclotron orbits in an external magnetic field. In the case when the orbit has an m-fold symmetry axis, the coordinate and momentum of the longitudinal motion of the electron contain harmonics of the cyclotron frequency that are multiples of m, since the longitudinal motion is modulated by the cyclotron rotation. Resonant interaction with the longitudinal wave arises under the condition $\omega = ms\Omega_{extr}$. Because of the modulation of the rotation of the electron, resonant interaction with the transverse waves arises at frequencies $\omega = (ms \pm 1)\Omega_{extr}$. It is these resonances which form the longitudinal and transverse anisotropons.

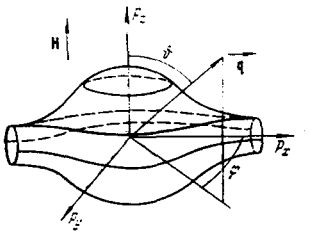

FIG. 10. Pinched-cylinder model of the Fermi surface. (Closed and open orbits and a self-intersecting trajectory are shown.)

Anisotropons in aluminum was studied in [86]. The spectrum of the right-polarized waves (which lies near the hole resonance $\Delta n = 5$) and that of the left-polarized waves (near the hole resonance $\Delta n = 3$) were calculated with a computer. The calculation showed that the departure of the initial frequency of the wave from the damping threshold amounts to a few per cent of the cyclotron frequency. The spectrum of the anisotropons is depicted schematically in Fig. 9.

Up to now we have considered resonances for electrons belonging to one part of the Fermi surface. Resonances at different parts of a multiply-connected Fermi surface can lead to the existence of additional transverse and longitudinal excitations. As already noted in Sec. 5(1), such waves have been studied theoretically and experimentally in bismuth.[61, 63]

3) We shall consider the electromagnetic excitations in metals with open Fermi surfaces in the presence of open orbits. First we shall analyze the condition for resonance absorption of a wave in metals with open Fermi surfaces in classically-strong magnetic fields. The motion in coordinate space corresponding to infinite motion of the electrons in momentum space in the direction of the p_x-axis is motion in the direction of the y-axis with average velocity $\bar{v}_y(p_z, p_y)$ (Fig. 10). The condition for resonance absorption therefore contains an additional term, proportional to $\bar{v}_y$:

$$\omega = \Delta n\Omega \pm \bar{v}_z \cos\vartheta q \pm \bar{v}_y \sin\vartheta \sin\varphi q. \tag{5.31}$$

The notation in (5.31) is clear from Fig. 10. The cyclotron frequency and the components $\bar{v}_y$ and $\bar{v}_z$ of the average velocity depend on p_z and p_y. Another feature of the

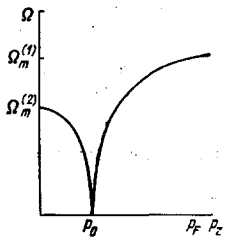

FIG. 11. Dependence of the cyclotron frequency on p_z in a magnetic field perpendicular to the axis of the pinched cylinder. (p_0 is the radius of the cylinder neck.)

situation considered is that the cyclotron frequency vanishes logarithmically at a certain value of p_z corresponding to a self-intersecting trajectory. A typical dependence of Ω on p_z is drawn in Fig. 11.

Let the wave-vector be perpendicular to the magnetic-field direction. For closed orbits the velocity $\bar{v}_y$ is equal to zero. Since the minimum cyclotron frequency is equal to zero, collisionless damping at closed-orbit electrons exists in the whole (ω, q)-plane. The thresholds in the damping for transitions with a fixed Δn are determined by the condition $\omega = \Delta n \Omega_{\max}^{(1)}$. The regions of damping at electrons belonging to open orbits also fill the whole (ω, q)-plane, for the same reason. However, the thresholds here are different:

$$\omega = \Delta n \Omega_{\max}^{(2)} \pm \tilde{v}_{y\max} \sin \varphi q, \qquad (5.32)$$

where $\tilde{v}_{y\max} = \hbar\Omega_{\max}^{(2)}/p_k \sim v_F$, $p_k = \hbar a_x/2l_H^2$ and a_x is the lattice constant in the x direction. The condition (5.32) points to the existence of resonance effects in the propagation of electromagnetic waves and sound.

Up to now, comparatively few papers have been published in which electromagnetic waves in metals with open Fermi surfaces, in the presence of open orbits, have been studied. As shown by Buchsbaum and Wolff, [80] the helicon and Alfven waves cannot propagate in such metals. This is explained by the fact that in the y direction, perpendicular to the open direction and to the magnetic-field direction, the average velocity of the electrons is not equal to zero and the conductivity σ_{yy} is finite in zeroth order in H^{-1} and does not depend on the magnetic field. The appearance of a large dissipative current in a direction perpendicular to the vector $\mathbf{q} \parallel \mathbf{H}$ leads to strong damping of these excitations.

The condition (5.32) for resonance absorption tells us the regions in the (ω, q)-plane in which the propagation of electromagnetic excitations is possible. Weakly-damped electromagnetic waves in metals in the presence of open orbits were studied in [87,88]. In the first of these, a model of the pinched-cylinder type was used as the model of the open Fermi surface and the solutions of the dispersion equation for a "normal" wave were found. It was found that the excitations propagating in the direction perpendicular to **H** and to the open direction have a spectrum that is confined near the thresholds (5.32). In [88], a corrugated-cylinder model consisting of slightly overlapping spheres was taken as the model. It was shown that, in the vicinity of the threshold of the Doppler-shifted cyclotron resonance (5.32) due to electrons on the open part of the Fermi surface, weakly-damped electromagnetic excitations, similar to dopplerons, can also exist. Unlike in [87], here the dispersion equation for excitations with the "wrong" polarization was solved and it was established that a doppleron localized near the threshold with $\Delta n = 1$ exists only under certain conditions on the electrons on the closed parts of the Fermi surface.

4) To investigate the spectrum of the electromagnetic excitations and the different resonance effects in quantizing magnetic fields in metals with an anisotropic Fermi surface, it is useful, as previously, to construct the collisionless-damping regimes and determine the singularities of the conductivity. Below we shall show that for a sufficiently complicated Fermi surface the magnetic quantization can lead to the appearance of new thresholds and can strengthen the conductivity singularities. We shall assume that the energy of a Bloch electron in the magnetic field is known and is a function of only two quantum numbers, n and p_z. For an arbitrary dispersion law $\varepsilon_n(p_z)$, as in the simplest model of the spectrum, collisionless-damping thresholds of three types should exist. One of these types corresponds to processes in which electrons from states with the Fermi momentum p_n, by absorbing a quantum of the field, undergo transitions to some state above the Fermi level, another corresponds to transitions from a state with momentum $-p_n$ to states with momentum greater than p_n, and the third is due to transitions from states below the Fermi level to a state with p_n.

In metals with an anisotropic spectrum, additional collisionless-damping thresholds can exist. We shall show this. For simplicity, we shall consider electron transitions with no change in the quantum number n. The corresponding contribution to the conductivity is proportional to

$$\int \frac{f_0[\varepsilon_n(p_z \pm \hbar q_z)] - f_0[\varepsilon_n(p_z)]}{\varepsilon_n(p_z \pm \hbar q_z) - \varepsilon_n(p_z) - \hbar\omega - i\delta}\, dp_z. \qquad (5.33)$$

Suppose that, for fixed ω and q, the denominator in (5.33) vanishes at a certain point p_z'. We expand the energy difference in (5.33) about this point, in a series in $\Delta p_z = p_z - p_z'$. If p_z' coincides with the limits of integration in (5.33) and the difference of the first derivatives in the expansion of the denominator is not equal to zero, then the real part of (5.33) has a logarithmic singularity. According to (5.33), the position of the logarithmic singularities is determined by the conditions

$$\hbar\omega = \varepsilon_n(p_n \pm \hbar q_z) - \varepsilon_n(p_n), \quad \hbar\omega = \varepsilon_n(p_n) - \tilde{\varepsilon}_n(p_n - \hbar q_z). \qquad (5.34)$$

These are the boundaries of the collisionless-damping regimes and correspond to the three absorption processes indicated above.

If the point p_z' is inside the region of integration and the difference of the first derivatives in it is equal to zero, the conductivity has a root singularity. The position of this threshold can be found from the equations

$$\varepsilon_n(p_z' + \hbar q_z) - \varepsilon_n(p_z') = \hbar\omega, \quad \frac{\partial \varepsilon_n(p_z' + \hbar q_z)}{\partial p_z} = \frac{\partial \varepsilon_n(p_z')}{\partial p_z} \qquad (5.35)$$

after eliminating p_z'. The threshold (5.35) corresponds to electron transitions from states below the Fermi level to states lying above the Fermi level, such that the electron velocities in the initial and final states are equal.

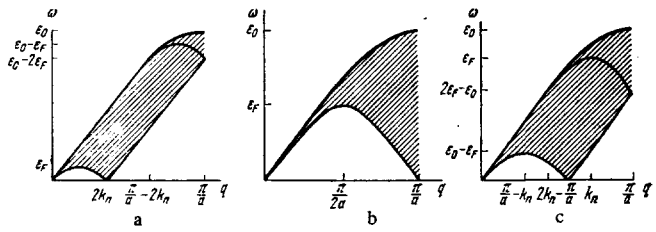

FIG. 12. Landau-damping regime in the model (5.36) of the electron spectrum. (The damping regimes corresponding to electron transitions in a weakly filled Landau level ($2k_n < \pi/a$) (Fig. 12a), a strongly filled level ($2k_n > \pi/a$) (Fig. 12c) and in a half-filled level ($2k_n = \pi/a$) (Fig. 12b). The conductivity has a logarithmic singularity on the damping boundaries represented by a thin line. On the boundaries represented by a thick line the singularity is of the root type.)

The reasoning given above is conveniently illustrated using the example of an electron spectrum of the corrugated-cylinder type (5.26), in a magnetic field directed along the axis of the cylinder:

$$\varepsilon_n(p_z) = \hbar\Omega\left(n+\frac{1}{2}\right) + \frac{\varepsilon_0}{2}\left(1-\cos\frac{p_z a}{\hbar}\right). \qquad (5.36)$$

Using the expressions (5.33)–(5.35), we shall determine the positions of the logarithmic and root singularities of the longitudinal conductivity. If the height of the Landau tube is less than half the size of the Brillouin zone, i.e., $k_n < \pi/2a$, then, as follows from (5.34), the Landau damping is not equal to zero in the range $\omega_- \leqslant \omega \leqslant \omega_+$, in which the threshold values of the frequency at which the conductivity has a logarithmic singularity are equal to

$$\omega_\pm = \omega_0(q)\left|\sin\left(k_n \pm \frac{1}{2}q\right)a\right|. \qquad (5.37)$$

For $q > (\pi/a) - 2k_n$, when the processes (5.35) become possible, a new Landau-damping regime $\omega_+ < \omega < \omega_0$ appears and the new root threshold is (Fig. 12a)

$$\omega_0(q) = \frac{\varepsilon_0}{\hbar}\left|\sin\frac{qa}{2}\right|. \qquad (5.38)$$

In the case when the height of the Landau tube is greater than half the size of the zone ($k_n > \pi/2a$), the Landau-damping boundaries at which the conductivity has a logarithmic singularity are determined by the expressions

$$\omega_\pm = \omega_0(q)\left|\sin\left(k_n \mp \frac{1}{2}q\right)a\right|. \qquad (5.39)$$

At the point $q = 2k_n - (\pi/a)$, as in the preceding case, the root threshold (5.38) splits off (see Fig. 12c). If the height of the Landau tube is equal to half the size of the zone, the root threshold starts at $q = 0$ (see Fig. 12b). We shall not give here the analytical expressions for the conductivity in the model (5.36). They are completely analogous to the expressions obtained in the recently published paper[89] for the conductivity of quasi-one-dimensional systems of the TCNQ type.

The principal result of the example given is that, in the region of small velocities v of the Bose excitations and of $q < |\pi/a - 2k_n|$, the behavior of the imaginary and real parts of the conductivity in metals with a fairly complicated spectrum is the same as in the model with $\varepsilon = p^2/2m$: the singularities of the nondissipative part of the conductivity are logarithmic while the discontinuities of the dissipative part are finite. Therefore, the character of the giant quantum oscillations in the absorption of sound or of a helicon in metals with an anisotropic Fermi surface is as before. The minimum velocities in the model (5.36) correspond to electrons at weakly and strongly occupied levels, i.e., to electrons at the extremal sections of the Fermi surface. However, in the propagation of excitations with velocities close to the maximum electron velocity, the resonances can be strengthened even in the region of small q. These resonances are associated with electrons in half-filled levels. The strengthening of the conductivity singularity can be reflected, e.g., in the spectrum of the fast magnetosonic wave in an inclined field, when $v_\alpha \sim v_F \cos\vartheta$.

Generally speaking, the energy of an electron in a quantizing magnetic field and in the periodic field of the lattice depends on three quantum numbers. This is valid in the case of both intraband and interband (cf., e.g., [90]) magnetic breakdown. If a closed orbit makes a close approach to the boundaries of the Brillouin zone, a tunneling transition from one orbit to another becomes possible. When the transition probability is small the energy depends only on n and p_z. If the transition probability is not small, then it is necessary to take into account the dependence of the energy on the third quantum number. This means that a certain range of energies corresponds to specific values of n and p_z—a Landau level is transformed into a magnetic band. For closed orbits the broadening of the Landau levels is exponentially small.[91] If there are open orbits in the metal, the spacing between the magnetic bands is exponentially small. In the intermediate region, corresponding to trajectories that approximate to a self-intersecting trajectory, the width of the magnetic band is of the order of the spacing between the Landau levels.

From what has been said, the character of the resonances for electrons corresponding to the three enumerated groups of orbits is clear. Resonances on closed trajectories with $\Delta n = 0$ and for $q \to 0$ correspond to narrow damping regions and broad areas of transparency. Trajectories lying close to a self-interesecting trajectory correspond to broader maxima in the absorption and narrower windows. Open orbits do not lead to singularities in the conductivity tensor. By varying the angle between the wave-vector of the electromagnetic wave or sound[92,93] and the magnetic-field direction, the different types of resonances can be successively observed in metals with open Fermi surfaces.

6. CONCLUDING REMARKS

In this review we have attempted to examine the spectrum of electromagnetic excitations in conductors in a strong magnetic field from a unified point of view. We have been interested chiefly in the origin of the characteristic electromagnetic modes and in their connection with the spectrum of Fermi excitations. An analysis of the conservation laws made it possible to

determine the positions of the different branches of the spectrum of electromagnetic excitations in the (ω, q)-plane and gave a natural classification of a number of resonance effects in the propagation of electromagnetic waves and other Bose excitations.

Despite the fact that the flow of papers in which electromagnetic excitations in metals and semimetals have been studied has not declined in recent years, a number of the waves have still not been observed experimentally. This applies primarily to the quantum electromagnetic waves. In the review, therefore, we have attempted to attract the attention of experimentalists to the as-yet unobserved electromagnetic excitations of a solid-state plasma.

The present state of the theory makes it possible to carry out a calculation of the spectrum of the electromagnetic waves in specific metals using realistic models of the Fermi surface. Evidently, the electromagnetic excitations in those metals in which the electron spectrum has been sufficiently fully investigated will be analyzed in detail in the next few years.

In metals with a simple electron dispersion law, from the theoretical point of view the detailed study of the resonance phenomena in the pre-threshold region is of extreme interest. Up to the present, threshold effects have been studied in the framework of the self-consistent field approximation. An exception is [94], in which, in a calculation of the vertex part and polarization operator in the pre-threshold region in a quantizing magnetic field, the principal logarithmically divergent diagrams in the perturbation theory series were summed.

Only resonance effects that are linear in the wave amplitude have been discussed in the review. With increase of the field amplitude the pattern of the threshold phenomena can change substantially. A number of theoretical [95–99] and experimental [100–102] papers have been devoted to the study of nonlinear resonance effects in strong magnetic fields. It should be noted that the approach used in this review for the analysis of linear resonance effects can also be useful for the study of nonlinear resonance phenomena.

The authors are grateful to E. A. Kaner and M. I. Kaganov for useful discussions.

APPENDIX

Here, following [25], we give a derivation of the conductivity tensor of an electron gas in a quantizing magnetic field. We shall seek the nonequilibrium density matrix in the form

$$\hat{\rho}=\hat{\rho}_0(\hat{\mathscr{H}}, \mu)+\hat{\rho}_1, \tag{A.1}$$

where

$$\hat{\rho}_0(\hat{\mathscr{H}}, \mu)=\rho_0(\hat{\mathscr{H}}_0, \mu_0)+\hat{\rho}_2. \tag{A.2}$$

The matrices $\hat{\rho}_1$ and $\hat{\rho}_2$ are linear in the amplitudes of the potentials $\mathbf{A}$ and ϑ, μ_0 is the equilibrium value of the chemical potential and $\hat{\rho}_0(\hat{\mathscr{H}}_0, \mu_0)$ is the density matrix at thermodynamic equilibrium. It is not difficult to convince oneself that in the representation defined by the operator $\hat{\mathscr{H}}_0$ (3.7) the matrix elements of the operator $\hat{\rho}_2$ are equal to

$$\langle\nu|\hat{\rho}_2|\nu'\rangle=\frac{f_0(\varepsilon_{\nu'})-f_0(\varepsilon_\nu)}{\varepsilon_{\nu'}-\varepsilon_\nu}\langle\nu|\hat{\mathscr{H}}_1-\mu_1|\nu'\rangle; \tag{A.3}$$

here,

$$\mu_1=\mu(\mathbf{r}, t)-\mu_0 \tag{A.4}$$

is the correction to the chemical potential, linear in the external field, and $f_0(\varepsilon_\nu)$ is the distribution function. Substituting (A1) into Eq. (3.3) and taking (3.10), (3.11) and (A2)–(A4) into account, we obtain

$$\langle\nu|\hat{\rho}|\nu'\rangle=f_0(\varepsilon_\nu)\delta_{\nu\nu'}+\Lambda_{\nu'\nu}\langle\nu|\hat{\mathscr{H}}_1-\mu_1|\nu'\rangle+\Lambda^{(1)}_{\nu'\nu}\langle\nu|\mu_1|\nu'\rangle, \tag{A.5}$$

where

$$\Lambda_{\nu'\nu}=\frac{i\omega\tau}{1+i\omega\tau}\Lambda^{(1)}_{\nu'\nu}+\frac{1}{1+i\omega\tau}\Lambda^{(2)}_{\nu'\nu}. \tag{A.6}$$

The matrices $\Lambda^{(1)}_{\nu'\nu}$ and $\Lambda^{(2)}_{\nu'\nu}$ are equal to

$$\Lambda^{(1)}_{\nu'\nu}=\frac{f_0(\varepsilon_{\nu'})-f_0(\varepsilon_\nu)}{\varepsilon_{\nu'}-\varepsilon_\nu-\hbar\omega+(i\hbar/\tau)}, \tag{A.7}$$

$$\Lambda^{(2)}_{\nu'\nu}=\frac{f_0(\varepsilon_{\nu'})-f_0(\varepsilon_\nu)}{\varepsilon_{\nu'}-\varepsilon_\nu}. \tag{A.8}$$

To calculate the current (3.4) it is necessary to calculate the trace. After a number of transformations and going over to the Fourier representation with respect to the space and time variables in (3.4), we obtain

$$j_i(\omega, \mathbf{q})=\frac{\omega_p^2}{4\pi c}\left[-A_i(\omega, \mathbf{q})-I_{ik}A_k(\omega, \mathbf{q})+K_i^{(1)}\varphi(\omega, \mathbf{q})+\frac{1}{e}(K_i-K_i^{(1)})\mu_1(\omega, \mathbf{q})\right]; \tag{A.9}$$

here $\omega_p^2=4\pi n_0 e^2/m$ is the square of the plasma frequency, n_0 is the concentration, N is the number of particles,

$$I_{ik}=\frac{2m}{N}\sum_{\nu'\nu}\Lambda_{\nu'\nu}\langle\nu'|V_i(\mathbf{q})|\nu\rangle\langle\nu'|V_k(\mathbf{q})|\nu\rangle^*, \tag{A.10}$$

$$\mathbf{V}(\mathbf{q})=\frac{1}{2}\exp(i\mathbf{qr})\hat{\mathbf{v}}_0+\frac{1}{2}\hat{\mathbf{v}}_0\exp(i\mathbf{qr}), \tag{A.11}$$

$$\mathbf{K}=\frac{2mc}{N}\sum_{\nu'\nu}\Lambda_{\nu'\nu}\langle\nu'|\mathbf{V}(\mathbf{q})|\nu\rangle\langle\nu'|\exp(i\mathbf{qr})|\nu^*\rangle, \tag{A.12}$$

$$K_i^{(\alpha)}=\frac{2mc}{N}\sum_{\nu'\nu}\Lambda^{(\alpha)}_{\nu'\nu}\langle\nu'|V_i(\mathbf{q})|\nu\rangle\langle\nu'|\exp(i\mathbf{qr})|\nu\rangle^*. \tag{A.13}$$

The matrix elements contained in these expressions have the following form:

$$\langle n', k_y+q_y, k_z+q_z|\exp(i\mathbf{qr})|n, k_y, k_z\rangle=f_{n'n}(q_y), \tag{A.14}$$

$$\langle n', k_y+q_y, k_z+q_z|V_x(\mathbf{q})|n, k_y, k_z\rangle=i\Omega\frac{\partial f_{n'n}(q_y)}{\partial q_y}, \tag{A.15}$$

$$\langle n', k_y+q_y, k_z+q_z|V_y(\mathbf{q})|n, k_y, k_z\rangle=\frac{\Omega}{q_y}(n'-n)f_{n'n}(q_y), \tag{A.16}$$

$$\langle n', k_y+q_y, k_z+q_z|V_z(\mathbf{q})|n, k_y, k_z\rangle=\frac{\hbar}{m}\left(k_z+\frac{q_z}{2}\right)f_{n'n}(q_y). \tag{A.17}$$

The function $f_{n'n}(q_y)$ is equal to

$$f_{n'n}(q_y)=\int_{-\infty}^{+\infty}dx\,u_{n'}(x+l_H^2q_y)\,u_n(x). \tag{A.18}$$

If $n'\geq n$, then

$$f_{n'n}=\sqrt{\frac{n!}{n'!}}\xi^{\frac{n'-n}{2}}\exp\left(-\frac{\xi}{2}\right)L_n^{n'-n}(\xi), \tag{A.19}$$

where $\xi=l_H^2q_y^2/2$ and L_n^α is a Laguerre polynomial. But if $n'<n$, we must use the relation

$$f_{n'n}=(-1)^{n-n'}f_{nn'}. \qquad \text{(A. 20)}$$

We return to the expression (A. 9) and eliminate μ_1 in it. By making use of (3.12), we have

$$\varphi(\omega,\ \mathbf{q})+\frac{1}{e}\mu_1(\omega,\ \mathbf{q})=\frac{c\tau\,(K_i^{(1)\prime}-K_i^{(2)\prime})\,E_i}{L_1+i\omega\tau L_2}, \qquad \text{(A. 21)}$$

$$K_i'(\omega-i\tau^{-1},\ \mathbf{q})=K_i^*(\omega+i\tau^{-1},\ \mathbf{q}), \qquad \text{(A. 22)}$$

$$L_\alpha=\frac{2mc^2}{N}\sum_{\nu\nu'}\Lambda^{(\alpha)}_{\nu'\nu}|\langle\nu'|\exp(i\mathbf{qr})\ \ \nu\rangle|^2. \qquad \text{(A. 23)}$$

After obvious transformations, having substituted $\mu_1(\omega, q)$ from (A. 21) into (A. 9), we write the current density in the following form:

$$j_i=(\sigma_{ik}+d_{ik})E_k, \qquad \text{(A. 24)}$$

$$\sigma_{ik}=\frac{\omega_p^2}{4\pi i\omega}(\delta_{ik}+I_{ik}), \qquad \text{(A. 25)}$$

$$d_{ik}=-\frac{\omega_p^2\tau}{4\pi(1+i\omega\tau)}\cdot\frac{(K^{(1)}-K^{(2)})_i\,(K'^{(1)}-K'^{(2)})_k}{L_1+i\omega\tau L_2}. \qquad \text{(A. 26)}$$

The term $d_{ik}E_k$ in (A. 24) is the density of the diffusion current, which vanishes as $\tau\to\infty$, and σ_{ik} is the conductivity tensor of the electron gas in a quantizing magnetic field. We give expressions for the nonzero components of the conductivity tensor and diffusion tensor for finite $\omega\tau$ in the symmetric geometry $\mathbf{q}\parallel\mathbf{H}$:

$$\sigma_\pm=\sigma_{xx}\mp i\sigma_{xy}=\frac{\omega_p^2}{4\pi i\omega}\left\{1+\frac{\hbar\Omega}{N(1+i\omega\tau)}\times\sum_{n,\,k_y,\,k_z}(n+1/2\pm1/2)\,[f_0(\varepsilon_{n\pm1,\,k_z+q_z})-f_0(\varepsilon_{n,\,k_z})]\times\left[\frac{i\omega\tau}{\varepsilon_n(k_z+q_z)-\varepsilon_n(k_z)-\hbar(\omega\mp\Omega-i\tau^{-1})}+\frac{1}{\varepsilon_n(k_z+q_z)-\varepsilon_n(k_z)\pm\hbar\Omega)}\right]\right\}, \qquad \text{(A. 27)}$$

$$\sigma_{zz}=\frac{\omega_p^2}{4\pi i\omega}\left\{1+\frac{2\hbar^2}{Nm(1+i\omega\tau)}\sum_{n,\,k_y,\,k_z}\left(k_z+\frac{q_z}{2}\right)^2[f_0(\varepsilon_{n,\,k_z+q_z})-f_0(\varepsilon_{n,\,k_z})]\times\left[\frac{i\omega\tau}{\varepsilon_n(k_z+q_z)-\varepsilon_n(k_z)-\hbar\omega-i\hbar\tau^{-1}}+\frac{1}{\varepsilon_n(k_z+q_z)-\varepsilon_n(k_z)}\right]\right\}, \qquad \text{(A. 28)}$$

$$d_{zz}=-\frac{i\omega\omega_p^2}{4\pi c^2q^2(\omega\tau)^2}\cdot\frac{L_1^2}{L_1+i\omega\tau L_2}, \qquad \text{(A. 29)}$$

$$L_1(\bar\omega,\ q)=\frac{mc^2}{N}\sum_{n,\,k_y,\,k_z}\frac{f_0[\varepsilon_n(k_z+q_z)]-f_0[\varepsilon_n(k_z)]}{\varepsilon_n(k_z+q_z)-\varepsilon_n(k_z)-\hbar\bar\omega}; \qquad \text{(A. 30)}$$

here $\bar\omega=\omega-i\tau^{-1}$ and $L_2=L_1(0, q)$. The nonzero components of the conductivity and diffusion tensors in another geometry ($\mathbf{q}\perp\mathbf{H}$) are given in [25]. A proof of the gauge invariance of the expressions cited is also given there.

[1]É. A. Kaner and V. G. Skobov, Adv. Phys. 17, 605 (1968).
[2]B. W. Maxfield, Am. J. Phys. 37, 241 (1969) (Russ. transl. Usp. Fiz. Nauk 103, 233 (1971)).
[3]J. Mertsching, Phys. Stat. Sol. 14, 3 (1966); 26, 9 (1968).
[4]V. S. Édel'man, Usp. Fiz. Nauk 102, 55 (1970) [Sov. Phys. Usp. 13, 583 (1971)].
[5]V. L. Ginzburg, Rasprostranenie élektromagnitnykh voln v plazme (The Propagation of Electromagnetic Waves in Plasmas), Fizmatgiz, M., 1960 (English translation published by Pergamon Press, Oxford, 1970).
[6]I. M. Lifshitz, M. Ya. Azbel' and M. I. Kaganov, Elektronnaya teoriya metallov (Electron Theory of Metals), Nauka, M., 1971 (English translation published by Consultants Bureau, N. Y., 1973).
[7]A. A. Abrikosov, Vvedenie v teoriyu normal'nykh metallov (Introduction to the Theory of Normal Metals), Nauka, M., 1973 (English translation—Solid State Physics, Supplement 12, Academic Press, N. Y., 1972).
[8]A. I. Akhiezer, I. A. Akhiezer, R. V. Polovin, A. G. Sitenko and K. N. Stepanov, Élektrodinamika plazmy (Electrodynamics of Plasmas), Nauka, M., 1974.
[9]P. M. Platzman and P. A. Wolff, Waves and Interactions in Solid-State Plasmas, Solid State Physics, Supplement 13, Academic Press, N. Y., 1973 (Russ. transl., Mir, M., 1975).
[10]I. A. Malkin and V. I. Man'ko, Zh. Eksp. Teor. Fiz. 55, 1014 (1968) [Sov. Phys. JETP 28, 527 (1969)].
[11]É. G. Bashkanskiĭ and A. P. Protogenov, Uch. zap. GGU (Gor'kiĭ State University), Ser. Fiz. 3, No. 126 (1971).
[12]V. G. Skobov and É. A. Kaner, Zh. Eksp. Teor. Fiz. 46, 1809 (1964) [Sov. Phys. JETP 19, 1219 (1964)].
[13]V. L. Gurevich, V. G. Skobov and Yu. A. Firsov, Zh. Eksp. Teor. Fiz. 40, 786 (1961) [Sov. Phys. JETP 13, 552 (1961)].
[14]A. Ya. Blank and É. A. Kaner, Zh. Eksp. Teor. Fiz. 50, 1013 (1960) [Sov. Phys. JETP 23, 673 (1966)].
[15]Yu. M. Gal'perin, Zh. Eksp. Teor. Fiz. 57, 551 (1969) [Sov. Phys. JETP 30, 302 (1970)].
[16]A. P. Protogenov and V. Ya. Demikhovskiĭ, Fiz. Tverd. Tela (Leningrad) 12, 3480 (1970) [Sov. Phys. Solid State 12, 2826 (1971)].
[17]V. Ya. Demikhovskiĭ and A. P. Protogenov, Zh. Eskp. Teor. Fiz. 58, 651 (1970) [Sov. Phys. JETP 31, 348 (1970)].
[18]V. Ya. Demikhovskiĭ and A. P. Protogenov, Fiz. Tverd. Tela (Leningrad) 12, 1963 (1970) [Sov. Phys. Solid State 12, 1561 (1971)].
[19]V. Ya. Demikhovskiĭ and V. M. Sokolov, Izv. AN SSSR Ser. Fiz. 36, 1518 (1962) [Bull. Acad. Sci. USSR, Phys. Ser.].
[20]V. Ya. Demikhovskiĭ, A. P. Protogenov and A. L. Chernov, Fiz. Metal. Metalloved. 33, 1129 (1972) [Phys. Metals. Metallog. (USSR) 33, No. 6, 7 (1972)].
[21]P. S. Zyryanov, V. I. Okulov and V. P. Silin, Pis'ma Zh. Eksp. Teor. Fiz. 8, 489 (1968); 9, 371 (1969) [JETP Lett. 8, 300 (1968); 9, 220 (1969)].
[22]P. S. Zyryanov, V. I. Okulov and V. P. Silin, Fiz. Metal. Metalloved. 28, 558 (1969) [Phys. Metals Metallog. (USSR) 28, No. 3, 187 (1969)].
[23]P. S. Zyranov, V. I. Okulov and V. P. Silin, Zh. Eksp. Teor. Fiz. 58, 1295 (1970) [Sov. Phys. JETP 31, 696 (1970)].
[24]P. S. Zyryanov and V. I. Okulov, Phys. Stat. Sol. 21, 89 (1967).
[25]J. Mertsching, Phys. Stat. Sol. 17, 799 (1966).
[26]M. P. Greene, H. J. Lee, J. J. Quinn, and S. Rodriguez, Phys. Rev. 177, 1019 (1969).
[27]V. I. Okulov, Fiz. Metal. Metalloved. 29, 924 (1970) [Phys. Metals Metallog. (USSR) 29, No. 5, 30 (1970)].
[28]E. N. Adams and T. D. Holstein, J. Phys. Chem. Sol. 10, 254 (1959).
[29]É. A. Kaner and V. G. Skobov, Zh. Eksp. Teor. Fiz. 53, 375 (1967) [Sov. Phys. JETP 26, 251 (1968)].
[30]J. J. Quinn and S. Rodriguez, Phys. Rev. 128, 2487 (1962).
[31]P. S. Zyryanov and V. P. Kalashnikov, Zh. Eksp. Teor. Fiz. 41, 1119 (1961) [Sov. Phys. JETP 14, 799 (1962)].
[32]S. L. Ginzburg, O. V. Konstantinov and V. I. Perel', Fiz. Tverd. Tela (Leningrad) 9, 2139 (1967) [Sov. Phys. Solid State 9, 1684 (1968)].
[33]O. V. Konstantinov and V. I. Perel', Zh. Eksp. Teor. Fiz. 53, 2034 (1967) [Sov. Phys. JETP 26, 1151 (1968)].
[34]A. L. McWhorter and W. May, IBM J. Res. and Dev. 8, 285 (1964).
[35]S. B. Anakhin and A. S. Kondrat'ev, Uch. Zap. LGU (Leningrad State University) No. 15, 25 (1968).
[36]P. S. Zyryanov, Zh. Eksp. Teor. Fiz. 40, 1065 (1961) [Sov. Phys. JETP 13, 751 (1961)].
[37]M. J. Stephen, Phys. Rev. 129, 997 (1963).
[38]V. Ya. Demikhovskiĭ and A. P. Protogenov, Fiz. Tverd. Tela (Leningrad) 11, 1173 (1969) [Sov. Phys. Solid State 11, 954 (1969)].
[39]M. E. Rensink, Phys. Rev. 174, 744 (1968).

[40]N. J. Horing, *ibid.* **186**, 434 (1969).
[41]O. V. Konstantinov and V. I. Perel', Zh. Eksp. Teor. Fiz. **38**, 161 (1960) [Sov. Phys. JETP **11**, 117 (1960)].
[42]A. J. Glick and E. Callen, Phys. Rev. **169**, 530 (1968).
[43]V. Ya. Demikhovskiĭ and A. P. Protogenov, Pis'ma Zh. Eksp. Teor. Fiz. **11**, 591 (1970) [JETP Lett. **11**, 409 (1970)].
[44]A. P. Protogenov, Zh. Eksp. Teor. Fiz. **62**, 313 (1972) [Sov. Phys. JETP **35**, 168 (1972)].
[45]É. A. Kaner and V. F. Gantmakher, Usp. Fiz. Nauk **94**, 193 (1968) [Sov. Phys. Usp. **11**, 81 (1968)].
[46]V. F. Gantmakher and É. A. Kaner, Zh. Eksp. Teor. Fiz. **45**, 1430 (1963) [Sov. Phys. JETP **18**, 988 (1964)].
[47]A. P. Protogenov and V. Ya. Demikhovskiĭ, Pis'ma Zh. Eksp. Teor. Fiz. **14**, 518 (1971) [JETP Lett. **14**, 356 (1971)].
[48]V. G. Veselago, M. V. Glushkov and L. V. Lyn'ko, Pis'ma Zh. Eksp. Teor. Fiz. **13**, 349 (1971) [JETP Lett. **13**, 247 (1971)].
[49]V. Ya. Demikhovskiĭ and A. P. Protogenov, Fiz. Tverd. Tela (Leningrad) **14**, 1948 (1972) [Sov. Phys. Solid State **14**, 1686 (1973)].
[50]D. Pines and J. R. Schrieffer, Phys. Rev. **124**, 1387 (1961).
[51]O. V. Konstantinov and V. I. Perel', Fiz. Tverd. Tela (Leningrad) **9**, 3051 (1967) [Sov. Phys. Solid State **9**, 2409 (1968)].
[52]C. C. Grimes, in: Proc. Symp. on Plasma Effects in Solids, Paris, 1964, p. 87.
[53]É. A. Kaner, I. I. Lyubimov and V. G. Skobov, Zh. Eksp. Teor. Fiz. **58**, 730 (1970) [Sov. Phys. JETP **31**, 391 (1970)].
[54]V. G. Skobov, Fiz. Tverd. Tela (Leningrad) **6**, 2297 (1964) [Sov. Phys. Solid State **6**, 1821 (1965)].
[55]É. A. Kaner and V. G. Skobov, Fiz. Tverd. Tela (Leningrad) **6**, 1104 (1964) [Sov. Phys. Solid State **6**, 851 (1964)].
[56]É. A. Kaner and V. G. Skobov, Physics **2**, 165 (1966).
[57]L. A. Fal'kovskiĭ, Usp. Fiz. Nauk **94**, 3 (1968) [Sov. Phys. Usp. **11**, 1 (1968)].
[58]M. H. Cohen and E. I. Blount, Phil. Mag. **5**, 115 (1960).
[59]L. É. Gurevich and R. G. Tarkhanyan, Fiz. Tekh. Poluprovodn. **3**, 1139 (1969) [Sov. Phys. Semicond. **3**, 962 (1970)].
[60]L. É. Gurevich and I. P. Ipatova, Zh. Eksp. Teor. Fiz. **37**, 1324 (1959) [Sov. Phys. JETP **10**, 943 (1960)].
[61]A. S. Garevskiĭ and V. Ya. Demikhovskiĭ, Fiz. Metal. Metalloved. **37**, 257 (1974) [Phys. Metals Metallog. (USSR) **37**, (1974)].
[62]É. A. Kaner and V. G. Skobov, Fiz. Tekh. Poluprovodn. **1**, 1367 (1967) [Sov. Phys. Semicond. **1**, 1138 (1968)].
[63]V. S. Edel'man, A. S. Garevskiĭ and V. Ya. Demikhovskiĭ, Fiz. Tverd. Tela (Leningrad) **16**, 3739 (1974) [Sov. Phys. Solid State **16**, 2435 (1975)].
[64]R. L. Blewitt and A. T. Sievers, J. Low Temp. Phys. **13**, 617 (1973).
[65]G. E. Smith, L. C. Hebel, and S. J. Buchsbaum, Phys. Rev. **129**, 154 (1963).
[66]É. A. Kaner and V. G. Skobov, Phys. Lett. **25A**, 105 (1967).
[67]P. K. Larsen and F. C. Greisen, Phys. Stat. Sol. **45**, 363 (1971).
[68]J. C. McGroddy, J. L. Stanford, and E. A. Stern, Phys. Rev. **141**, 431 (1966).
[69]A. W. Overhauser and S. Rodriguez, Phys. Rev. **141**, 431 (1966).
[70]L. M. Fisher, V. V. Lavrova, V. A. Yudin, O. V. Konstantinov and V. G. Skobov, Zh. Eksp. Teor. Fiz. **60**, 759 (1971) [Sov. Phys. JETP **33**, 410 (1971)].
[71]D. S. Falk, B. Gerson, and J. F. Carolan, Phys. Rev. **B1**, 406 (1970).
[72]R. G. Chambers, Phil. Mag. **1**, 459 (1956).
[73]R. G. Chambers and V. G. Skobov, J. Phys. **F1**, 202 (1971).
[74]A. W. Overhauser, Phys. Rev. Lett. **13**, 190 (1964).
[75]O. V. Konstantinov, V. G. Skobov, V. V. Lavrova, L. M. Fisher and V. A. Yudin, Zh. Eksp. Teor. Fiz. **63**, 224 (1972) [Sov. Phys. JETP **36**, 118 (1973)].
[76]V. P. Naberezhnykh, D. E. Zherebchevskii, L. T. Tsymbal, T. M. Yeryomenko, Sol State Comm. **11**, 1529 (1972).
[77]R. W. Stark and L. M. Falicov, Phys. Rev. Lett. **19**, 795 (1967).
[78]R. C. Jones, R. G. Goodrich and L. M. Falicov, Phys. Rev. **174**, 672 (1968).
[79]V. V. Lavrova, S. V. Medvedev, V. G. Skobov, L. M. Fisher, A. S. Chernov and V. A. Yudin, Zh. Eksp. Teor. Fiz. **66**, 700 (1974) [Sov. Phys. JETP **39**, 338 (1974)].
[80]S. J. Buchsbaum and P. A. Wolff, Phys. Rev. Lett. **15**, 406 (1965).
[81]B. Perrin, G. Weisbuch, and A. Libchaber, Phys. Rev. **B1**, 1501 (1970).
[82]V. G. Skobov, L. M. Fisher, A. S. Chernov and V. A. Yudin, Zh. Eskp. Teor. Fiz. **67**, 1218 (1974) [Sov. Phys. JETP 40, 605].
[83]V. V. Lavrova, V. G. Skobov, L. M. Fisher, A. S. Chernov and V. A. Yudin, Fiz. Tverd. Tela (Leningrad) **15**, 3379 (1973) [Sov. Phys. Solid State **15**, 2245 (1974)].
[84]O. V. Konstantinov and V. G. Skobov, Fiz. Tverd. Tela (Leningrad) **12**, 2768 (1970) [Sov. Phys. Solid State **12**, 2237 (1971)].
[85]O. V. Konstantinov and V. G. Skobov, Zh. Eksp. Teor. Fiz. **61**, 1660 (1971) [Sov. Phys. JETP **34**, 885 (1972)].
[86]V. Ya. Demikhovskiĭ and S. S. Savinskiĭ, Zh. Eksp. Teor. Fiz. (1976) [Sov. Phys. JETP (1976)].
[87]A. P. Protogenov and V. E. Sautkin, Pis'ma Zh. Eksp. Teor. Fiz. **17**, 324 (1973) [JETP Lett. **17**, 233 (1973)].
[88]É. A. Kaner and O. I. Lyubimov, Zh. Eksp. Teor. Fiz. **65**, 778 (1973) [Sov. Phys. JETP **38**, 386 (1974)].
[89]P. F. Williams and A. N. Bloch, Phys. Rev. **B10**, 1097 (1974).
[90]A. A. Slutskin and S. A. Sokolov, Pis'ma Zh. Eksp. Teor. Fiz. **14**, 60 (1971) [JETP Lett. **14**, 40 (1971)].
[91]G. E. Zil'berman, Zh. Eksp. Teor. Fiz. **33**, 387 (1957) [Sov. Phys. JETP **6**, 299 (1958)].
[92]Yu. M. Gal'perin, S. V. Gantsevich and V. L. Gurevich, Zh. Eksp. Teor. Fiz. **56**, 1728 (1969) [Sov. Phys. JETP **29**, 926 (1969)].
[93]Yu. M. Gal'perin, Fiz. Tverd. Tela (Leningrad) **11**, 1710 (1969) [Sov. Phys. Solid State **11**, 1385 (1969)].
[94]S. A. Brazovskiĭ, Zh. Eksp. Teor. Fiz. **61**, 2401 (1971) [Sov. Phys. JETP **34**, 1286 (1972)].
[95]Yu. M. Gal'perin and V. D. Kagan, Fiz. Tverd. Tela (Leningrad) **10**, 2037 (1968) [Sov. Phys. Solid State **10**, 1600 (1969)].
[96]Yu. M. Gal'perin and V. I. Kozub, Zh. Eksp. Teor. Fiz. **63**, 1083 (1972) [Sov. Phys. JETP **36**, 570 (1973)].
[97]Yu. I. Balkarei and É. M. Epshtein, Zh. Eksp. Teor. Fiz. **63**, 660 (1972) [Sov. Phys. JETP **36**, 349 (1973)].
[98]V. Ya. Demikhovskiĭ and A. P. Kopasov, Zh. Eksp. Teor. Fiz. **64**, 1007 (1973) [Sov. Phys. JETP **37**, 512 (1973)].
[99]A. P. Kopasov and V. Ya. Demikhovskiĭ, Fiz. Tverd. Tela (Leningrad) **15**, 3589 (1973) [Sov. Phys. Solid State **15**, 2395 (1974)].
[100]W. Salaneck, Y. Sawada, and E. Burstein, J. Phys. Chem. Sol. **32**, 2285 (1971).
[101]A. P. Korolyuk and V. F. Roĭ, Pis'ma Zh. Eksp. Teor. Fiz. **17**, 184 (1973) [JETP Lett. **17**, 131 (1973)].
[102]A. P. Korolyuk, V. I. Khotkevich, M. A. Obolenskii and V. I. Beletskiĭ, Pis'ma Zh. Eksp. Teor. Fiz. **18**, 32 (1974) [JETP Lett. **18**, 17 (1974)].

Translated by P. J. Shepherd